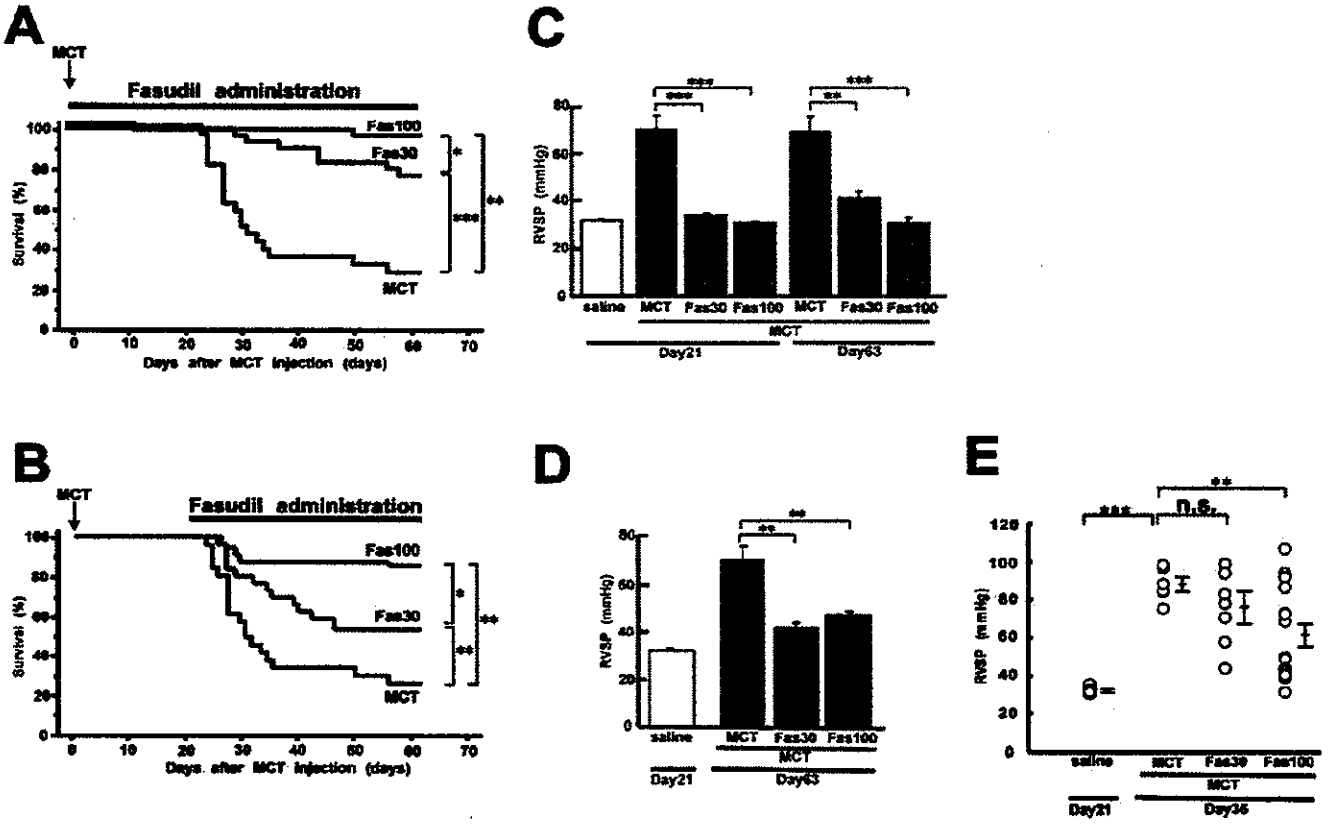

Figure 1. Fasudil improves survival of rats with MCT-induced PH. Compared with the saline-treated normal group (saline), in both the prevention (top) and treatment (bottom) protocols, the fasudil treatment markedly improved the survival (A and B) and RV systolic pressure (C and D). At day 35 (14 days after MCT injection), fasudil already started reducing RVSP in the treatment protocol in a dose-dependent manner (E). Fas 30 and 100; fasudil 30 and 100 mg/kg per day, orally, respectively. $^{*}P<0.05$, $^{**}P<0.01$, $^{***}P<0.0001$. n.s. indicates not statistically significant.

dependently improved the survival: 53% in the low-dose (n=30) and 86% in the high-dose (n=35) groups (Figure 1B).

Improvement of PH and RVH by Fasudil

The MCT group developed severe PH at day 21 with increased RV systolic pressure (a marker of systolic pulmonary pressure) compared with the sham-operated saline-treated group (Figures 1C and 1D). In the prevention protocol, fasudil markedly and dose-dependently suppressed the development of PH at day 21 in both the low-dose and the high-dose groups, the effects of which were maintained at day 63 (Figure 1C). In the treatment protocol, fasudil caused a marked regression of the MCT-induced PH at day 63 (Figure 1D). In this protocol, we also measured RV systolic pressure at day 35 in the middle of the experiment in some animals separately before they died. The results showed that fasudil had started reducing RV systolic pressure in a dose-dependent manner (Figure 1E). Mean systemic arterial pressure (mm Hg) was significantly decreased in the MCT group (75±2, n=6) compared with the saline-treated group (115±2, n=6, $P<0.0001$). In the prevention protocol, fasudil prevented the reduction in systemic arterial pressure in the low-dose and the high-dose groups at day 21 (113±4 and 117±1, respectively, n=6 each) compared with the MCT alone group. In the treatment protocol, fasudil again improved the arterial pressure in the low-dose and the high-dose groups at day 63 (121±4 and 121±3, respectively, n=6 each). In the MCT group, a significant RVH was developed, and fasudil markedly suppressed the MCT-induced RVH in the prevention protocol (Figure 2A) and caused a marked regression of RVH in the treatment protocol (Figure 2B).

We also measured the extent of RVH in animals that died in the middle of the experiments. The measurement was performed within 12 hours after death in all animals. The extent of RVH in dead animals of the MCT group was 0.74±0.06 (n=7) with a pleural effusion and ascites. In the dead animals in the prevention protocol with fasudil, a similar extent of RVH was noted in both the low-dose (0.67±0.08, n=4) and the high-dose (0.72, n=1) groups with a pleural effusion and ascites. Similarly, the dead animals in the treatment protocol also showed marked RVH in both the low-dose (0.68±0.05, n=9) and the high-dose (0.71±0.04, n=3) groups with a pleural effusion and ascites.

Inhibitory Effects of Fasudil on Medial Wall Thickening

Medial thickness was markedly increased in the MCT group compared with the saline-treated group or the fasudil-treated groups (Figures 3A through 3D). We semiquantitatively evaluated the extent of muscularization of pulmonary microvessels (15 to 50 μm in diameter) because they are usually nonmuscular under normal conditions. In the prevention protocol, at both day

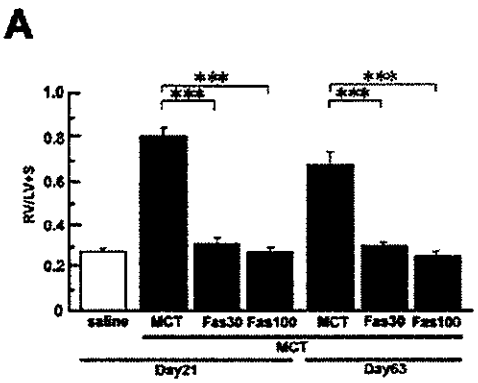

Figure 2. Fasudil improves RV hypertrophy in rats with MCT-induced PH. Compared with the saline-treated normal group (saline), in both the prevention (A) and treatment (B) protocols, the fasudil treatment markedly improved MCT-induced RV hypertrophy. Fas 30 and 100; fasudil 30 and 100 mg/kg per day, orally, respectively. ***$P<0.0001$.

21 and day 63, fasudil prevented the muscularization at both a low-dose and a high-dose at day 21 and day 63 (Figure 3E). In the treatment protocol, fasudil markedly improved the muscularization at both doses at day 63 (Figure 3F).

We next quantified medial wall thickness of pulmonary arteries in the ranges of 50 to 100 μm and 101 to 200 μm in diameter separately. In the prevention protocol, fasudil prevented the MCT-induced medial thickening of both-sized pulmonary arteries at both day 21 and day 63 (Figures 3G and 3I). In the treatment protocol, fasudil caused a marked improvement of the MCT-induced medial thickening of both-sized pulmonary arteries at day 63 (Figures 3H and 3J).

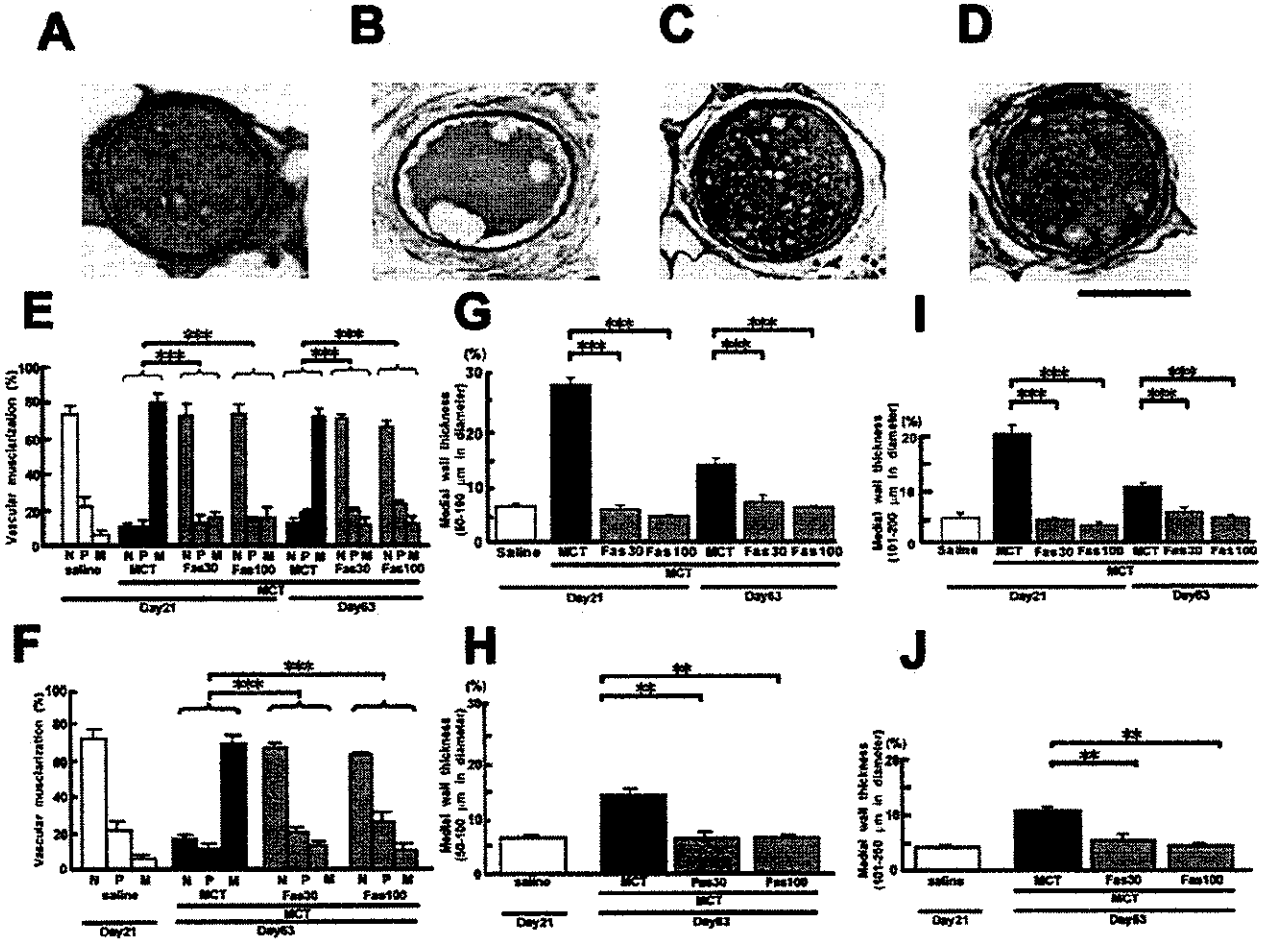

Figure 3. Fasudil suppresses medial thickening in rats with MCT-induced PH. Compared with the saline-treated normal group (A), medial wall thickening of the pulmonary artery was noted in the MCT group (B), whereas fasudil prevented (C) or markedly improved the medial thickening (D). Bar=50 μm. In the prevention protocol (middle), the fasudil treatment markedly suppressed the MCT-induced muscularization of pulmonary microvessels (15 to 50 μm in diameter) (E) as well as percent medial wall thickening of pulmonary arteries at both 50 to 100 μm (G) and 101 to 200 μm levels (I). In the treatment protocol (bottom), the fasudil treatment induced a marked improvement of the vascular muscularization of pulmonary microvessels (15 to 50 μm diameter) (F) and percent medial wall thickening of pulmonary arteries at both 50 to 100 μm (H) and 101 to 200 μm levels (J). N indicates nonmuscular; P, partially muscular; M, muscular. Results are expressed as mean±SEM (n=3 each). **$P<0.01$, ***$P<0.0001$.

Mechanisms for the Beneficial Effects of Fasudil on PH

PCNA expression in VSMCs was increased in the MCT group at day 21, which was prevented by fasudil (Figures 4A through 4C and 4J). Fasudil also significantly enhanced VSMC apoptosis (Figures 4D through 4F and 4K). The percentage of TUNEL-positive cells was significantly increased in the fasudil group compared with the saline-treated normal group and the MCT group (Figure 4K). Macrophage recruitment was increased in the MCT group, which was also markedly suppressed by fasudil (Figures 4G through 4I and 4L).

Endothelium-dependent relaxation of isolated pulmonary arteries to ACh was markedly impaired in the MCT group, which was prevented by fasudil (Figure 5A). This beneficial effect of fasudil was abolished by L-NNA (Figure 5B). Serotonin caused hypercontractions of pulmonary VSMC from the MCT group, which was prevented by the fasudil treatment and also by the acute administration of hydroxyfasudil (Figure 5C). Endothelium-independent relaxation to SNP also was slightly but significantly impaired in the MCT group, which was again prevented by the fasudil treatment (Figure 5D).

The extent of ERM phosphorylation was significantly increased in the MCT group and was markedly inhibited by the fasudil treatment (Figure 6A). The expression of eNOS in the lungs was significantly increased by the fasudil treatment (Figure 6B).

Plasma Concentration of Hydroxyfasudil

The mean value of the daily plasma concentration of hydroxyfasudil (AUC_{0-24}, ng/hr per mL) in rats that received fasudil in drinking water was 627 and 1450 for the low-dose (30 mg/kg per day) and the high-dose (100 mg/kg per day) groups, respectively (n=4 each).

Discussion

The novel findings of the present study were that the Rho-kinase–mediated pathway is substantially involved in the MCT-induced PH and that the long-term inhibition of Rho-kinase with fasudil prevents or even causes a marked improvement of the MCT-induced PH through multiple mechanisms, including (1) inhibition of VSMC proliferation with enhanced apoptosis, (2) reduced macrophage infiltration, and (3) improvement of endothelium-dependent relaxation and VSMC hypercontraction (Figure 7).

Rho-Kinase in the MCT-Induced PH Model

MCT is known to cause endothelial injury of pulmonary arteries with subsequent proliferation of pulmonary VSMC and infiltration of inflammatory cells.[3,18] Accumulating evidence indicates that Rho-kinase–mediated pathway is involved in the vascular effects of various vasoactive substances, including angiotensin II,[26] endothelin-1,[27] and serotonin,[15] all of which may be involved in the pathogenesis of PH.[28–30] We also have recently demonstrated that inflammatory stimuli (eg, angiotensin II and IL-β) upregulate Rho-kinase in human coronary VSMCs.[31] Those inflammatory processes may activate Rho-kinase in this MCT-induced PH model. Thus, Rho-kinase may play an important role in the pathogenesis of PH both directly, by activating its substrates, and indirectly, by mediating the signal transduction of various inflammatory mediators.

Recently, it has been reported that simvastatin, which also could inhibit Rho/Rho-kinase signaling, inhibits both hypoxia-induced and MCT-induced PH.[32–35] Nagaoka et al[36] also have reported that chronic hypoxia-induced PH is almost completely reversed by acute inhibition of Rho-kinase in rats. These reports also suggest that Rho-kinase signaling plays an important role in the pathogenesis of both hypoxia-induced and MCT-induced PH.

Hydroxyfasudil as a Specific Rho-Kinase Inhibitor

Hydroxyfasudil, an oral metabolite of fasudil, is a specific Rho-kinase inhibitor.[13] In the present study, the mean value of the AUC_{0-24} of hydroxyfasudil in the fasudil group was within its clinical therapeutic range in humans (unpublished data, 2003). In our series of experiments, the extent of the increase in Rho-kinase activity as evaluated by that of ERM phosphorylation was 1.5- to 2.0-fold.[19,31,37,38] This Rho-kinase activity just represents the whole Rho-kinase activity in blood vessels, and it is highly possible that Rho-kinase activity may be much greater in activated cells (eg, inflammatory cells) but much less in others (eg, fibroblasts). We consider that Rho-kinase has multiple stimulatory effects on vascular lesion formation with this extent of activation (Figure 7), thus accelerating the process of PH.

In the present study, neither acute nor chronic administration of fasudil lowered systemic arterial pressure, indicating that the Rho-kinase inhibitor caused selective vasodilatation of pulmonary arteries.

Rho-Kinase and VSMC Proliferation and Apoptosis in PH

In our animal models of coronary arteriosclerosis, long-term treatment with fasudil suppressed coronary VSMC proliferation.[11–17] Rho-kinase is involved in VSMC cytokinesis as well as gene expression of many atherogenic molecules that stimulate VSMC proliferation.[8,10,11,37–39] Rho-kinase may affects various cyclin-dependent kinases.[26,31] In this study, fasudil also significantly enhanced apoptosis, a finding consistent with our recent study.[37] In the present study, established PH was improved to the normal level at day 63 with the fasudil treatment. Indeed, the long-term treatment with fasudil induced a marked improvement of medial wall thickening of pulmonary arteries partly due to its enhancing effect on VSMC apoptosis.

Rho-Kinase and Inflammatory Cell Migration in PH

Rho-kinase also is involved in inflammatory cell migration.[11,40] We previously demonstrated that long-term treatment with fasudil suppresses chemokine-induced migration of macrophages in porcine coronary arteries in vivo.[17] Macrophage recruitment has been implicated in the pathogenesis of PH because various vasoactive factors may be released from infiltrating inflammatory cells, especially macrophages, in pulmonary arteries.[3] Macrophages may be the most impacted by fasudil, followed by VSMC and endothelial cells. The present

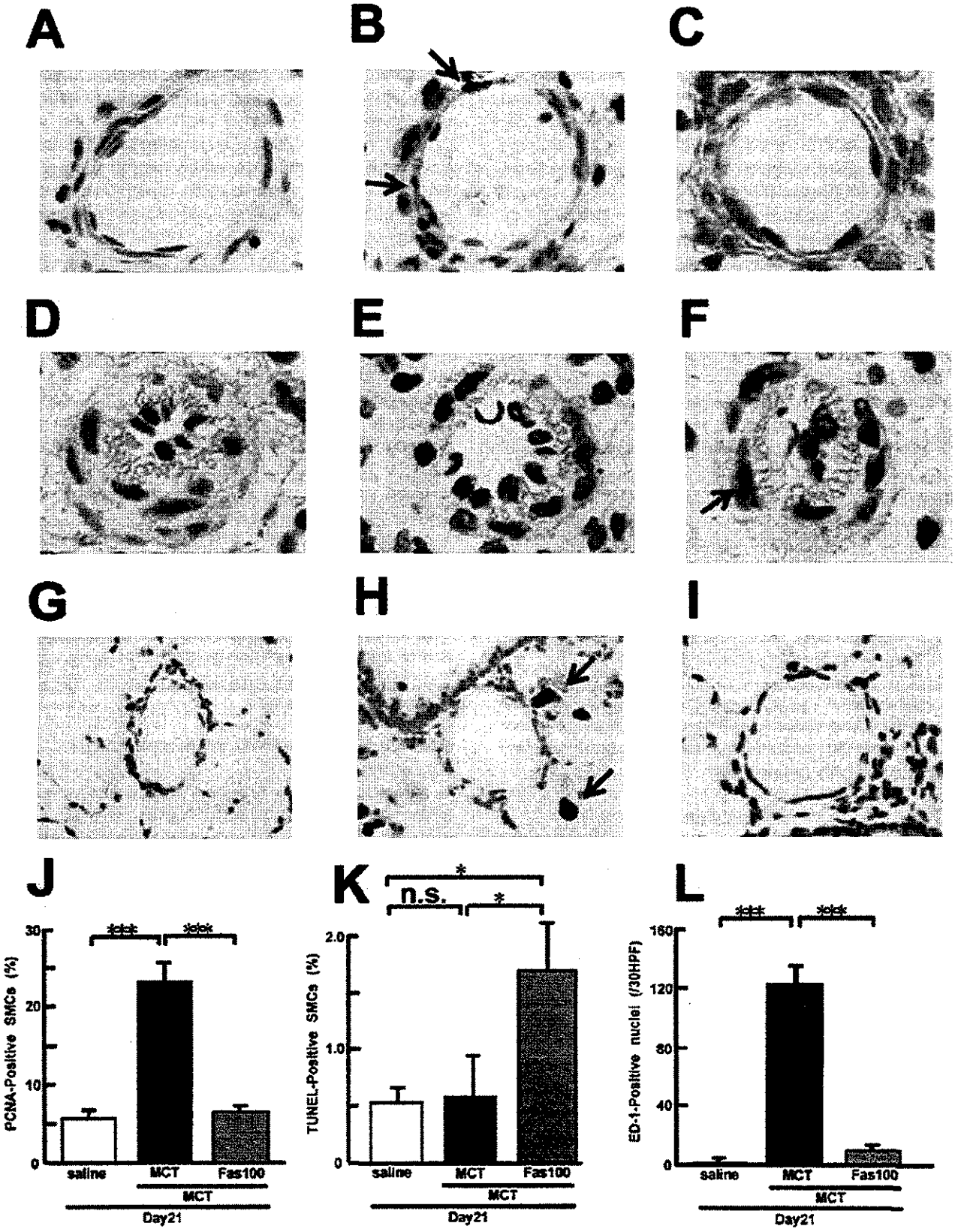

Figure 4. Mechanisms for the beneficial effects of fasudil on MCT-induced pulmonary remodeling. Histology of pulmonary arteries in the saline-treated normal group (A, D, and G), MCT group (B, E, and H), and high-dose fasudil group (C, F, and I) at day 21 in the prevention protocol. MCT-induced increase in PCNA-positive cells (arrows) was prevented in the fasudil group (A through C and J). TUNEL-positive cells (arrows) were increased in the fasudil group (D through F and K). MCT-induced increase in ED-1–positive macrophages (arrows) was prevented in the fasudil group (G through I and L). Results are expressed as mean±SEM (n=4 each). *P<0.05, ***P<0.0001. n.s. indicates not statistically significant.

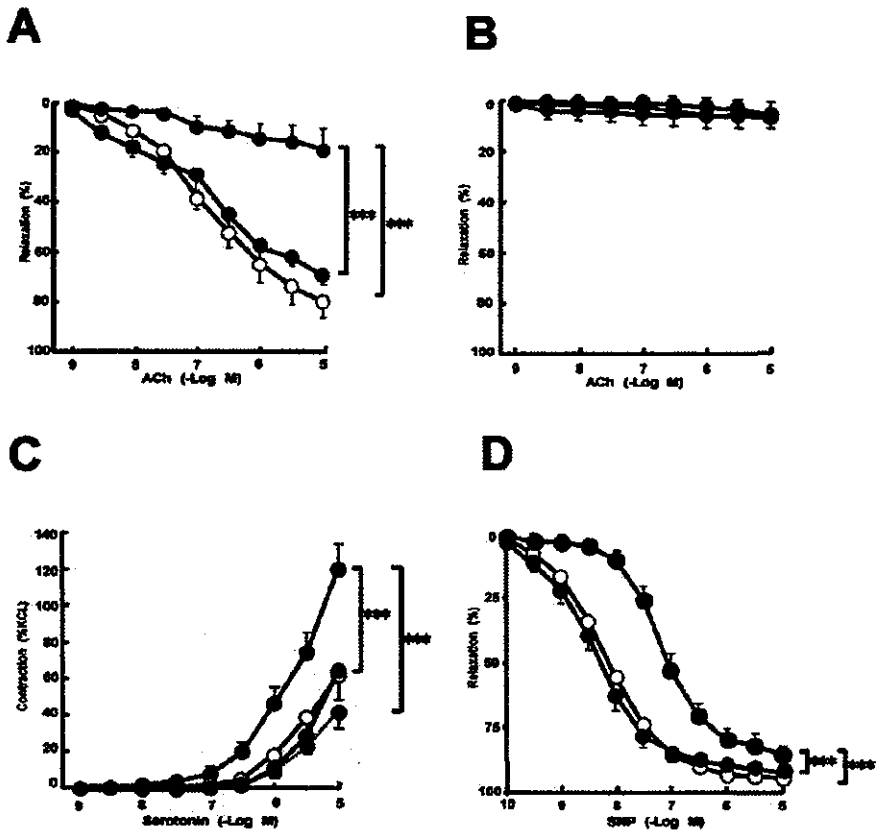

Figure 5. Fasudil improves endothelial and VSMC functions in rats with MCT-induced PH. A, MCT-induced endothelial dysfunction was markedly improved by the fasudil treatment at day 21 in the prevention protocol. B, Beneficial effect of fasudil was abolished by L-NNA (10^{-5} mol/L). C, Fasudil treatment significantly inhibited MCT-induced VSMC hypercontraction in response to serotonin (in rings without endothelium), as did acute administration of hydroxyfasudil (10^{-5} mol/L). D, Fasudil treatment improved the relaxation to sodium nitroprusside (SNP) in rings without endothelium compared with the MCT group. Open circle indicates saline-treated normal group; black circle, MCT-treated group; gray circle, fasudil-treated group; and black circle/dashed line, acute administration of hydroxyfasudil. Results are expressed as mean±SEM (n=6 to 7 each). ***$P<0.0001$.

study suggests that Rho-kinase–mediated macrophage recruitment also is involved in the pathogenesis of PH.

Rho-Kinase and Impaired Endothelium-Dependent Relaxation in PH

MCT causes endothelial injury and subsequent endothelial dysfunction of pulmonary arteries.[41] Impaired endothelium-dependent relaxation is caused by endothelial dysfunction and/or reduced VSMC vasodilator function. The present results demonstrate that both mechanisms are involved in the impaired endothelium-dependent relaxation in the MCT-induced PH. Regarding the endothelial dysfunction, a reduced NO bioactivity is involved as endothelium-dependent relaxation to ACh was totally mediated by NO in both the control and the fasudil-treated groups.[42] Regarding the VSMC dysfunction, endothelium-independent relaxation of VSMC to SNP was slightly but significantly impaired in the control group. Importantly,

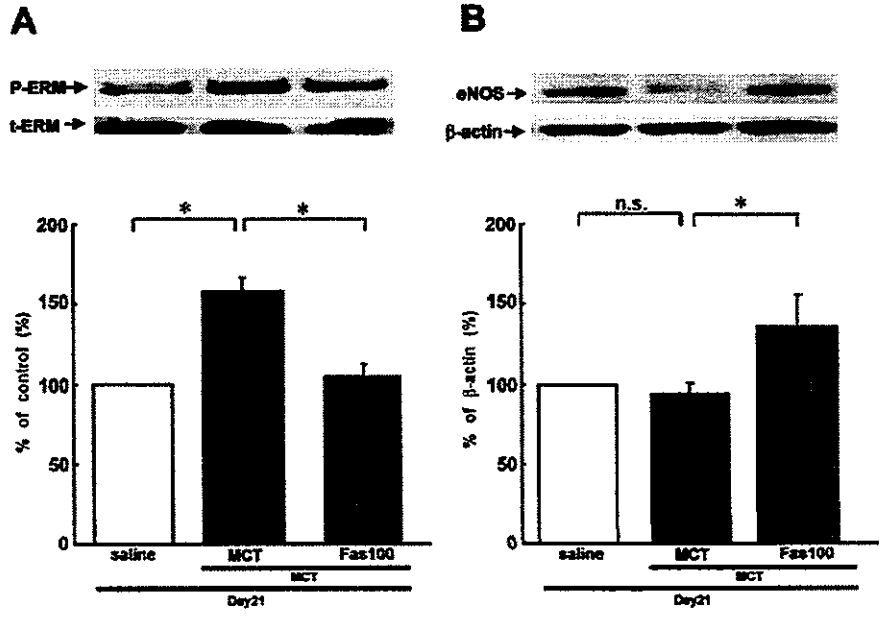

Figure 6. Effects of long-term treatment with fasudil on Rho-kinase activity eNOS expression in rats with MCT-induced PH. A, Compared with the saline-treated normal group, Rho-kinase activity, as evaluated by the extent of phosphorylation of the ERM family of pulmonary arteries, was significantly increased in the MCT group, which was significantly suppressed by the fasudil treatment at day 21 in the prevention protocol. P-ERM indicates phosphorylated ERM; t-ERM, total ERM. B, Fasudil treatment significantly increased eNOS expression of the lung at day 21 in the prevention protocol. eNOS level is shown as percent of the internal control β-actin level. Results are expressed as mean±SEM (n=3 to 5 each). *$P<0.05$. n.s. indicates not statistically significant.

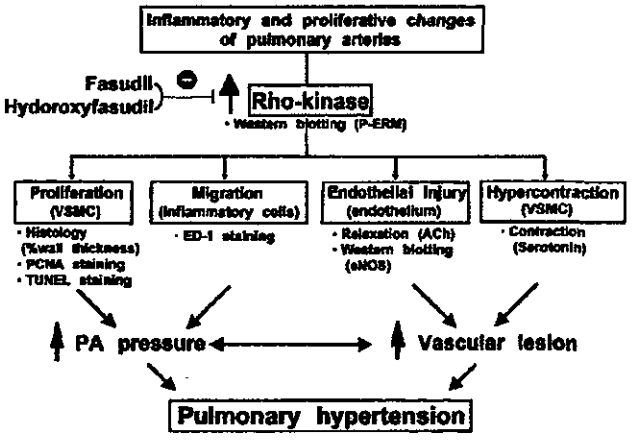

Figure 7. Summary of the present study. Multiple mechanisms appear to be involved in the pathogenesis of PH, all of which may be substantially mediated by Rho-kinase. Thus, the long-term blockade of Rho-kinase with fasudil or other Rho-kinase inhibitors may be useful for the treatment of PH.

the fasudil treatment improved both endothelial and VSMC dysfunction.

Recently, it was shown that sildenafil may be useful for the treatment of PH for its enhancing effect on NO-mediated vasodilatation.[43] We also have recently demonstrated that hydroxyfasudil prevents hypoxia-induced downregulation of eNOS.[23] In the present study, fasudil significantly upregulated eNOS expression. It is important to note that any pharmacological treatment that is effective in this PH model is associated with upregulation of eNOS.[24,25,42]

Rho-Kinase and VSMC Hypercontraction in PH

In the present study, VSMC contraction to serotonin was significantly enhanced in the MCT group, which may be involved in the increased pulmonary vascular resistance in the MCT-induced PH. We have demonstrated that Rho-kinase–mediated pathway plays a central role in the pathogenesis of VSMC hypercontraction or vasospasm in both porcine models and patients with vasospastic angina through inhibition of myosin phosphatase with subsequent enhancement of myosin light-chain phosphorylations.[11,13,16] Robertson et al[44] also reported that Y-27632, another specific Rho-kinase inhibitor, suppresses hypoxia-induced vasoconstriction in rats. Fasudil may improve endothelial and VSMC function in a different way in the present study. In endothelial cells, fasudil improved NO-mediated endothelial vasodilator function partly through augmentation of endothelial eNOS expression.[23] By contrast, in VSMCs, fasudil directly inhibited the Rho-kinase–mediated hypercontractions in a NO-independent manner as both acute and chronic treatment with fasudil abolished the VSMC hypercontractions. Recently, Sauzeau et al[45] have reported that hypoxia-induced PH is associated with downregulation of RhoA expression and decreased contractility of conduit pulmonary arteries. It remains to be examined in future studies if and how RhoA expression and activity are altered in PH.

Limitations of the Study

Several limitations should be mentioned for the present study. First, MCT-induced PH model may not fully represent PPH in humans and thus the usefulness of Rho-kinase inhibitors should be examined in other PH models with different etiologies. However, it has been reported that Rho-kinase signaling also plays an important role in hypoxia-induced pulmonary vasoconstriction.[46] We also have recently observed that long-term inhibition of Rho-kinase with fasudil suppresses hypoxia-induced PH in mice.[47] These results suggest that Rho-kinase signaling is substantially involved in the pathogenesis of PH with different etiologies. However, like other drugs that have been reported to attenuate experimental PH (eg, statins, rapamycin),[33,34,48] fasudil needs to be tested in the clinical setting. Second, some animals died in the fasudil groups. The cause of death appears to be RV failure due to PH even in the fasudil groups, suggesting that the fasudil treatment was not effective in all animals. It thus remains to be examined why fasudil was quite effective in some animals but not in others although the animals were genetically homogenous. Third, the mechanisms for the beneficial effects of fasudil were examined only in the prevention protocol due to the limited availability of the animals. However, it is conceivable that the same mechanisms of fasudil are involved in the treatment protocol.

Clinical Implications

PPH continues to be a serious clinical problem with high morbidity and mortality. We have recently confirmed the effectiveness and safety of oral administration of fasudil in patients with stable effort angina.[49] The present study suggests that Rho-kinase could be a novel therapeutic target for the treatment of PH in humans.

Acknowledgments

This study was supported in part by grants-in-aid (Nos. 12032215, 12470158, 12877114, 13307024, and 13557068) and a grant for the 21st Century COE Program from the Japanese Ministry of Education, Culture, Sports, Science and Technology, Tokyo, Japan, and the Program for Promotion of Fundamental Studies in Health Sciences of the Organization for Pharmaceutical Safety and Research of Japan. We thank M. Sonoda, I. Kunihiro, and E. Gunshima for excellent technical assistance and Asahi Kasei Corp (Tokyo, Japan) for providing fasudil. K.A. won the 2002 Best Abstract Award of the Pulmonary Circulation Council of the American Heart Association for this study.

References

1. Rabinovitch M. Pulmonary hypertension: updating a mysterious disease. *Cardiovasc Res.* 1997;34:268–272.
2. Rubin LJ. Cellular and molecular mechanisms responsible for the pathogenesis of primary pulmonary hypertension. *Pediatr Pulmonol Suppl.* 1999;18:194–197.
3. Kimura H, Kasahara Y, Kurosu K, Sugito K, Takiguchi Y, Terai M, Mikata A, Natsume M, Mukaida N, Matsushima K, Kuriyama T. Alleviation of monocrotaline-induced pulmonary hypertension by antibodies to monocyte chemotactic and activating factor/monocyte chemoattractant protein-1. *Lab Invest.* 1998;78:571–581.
4. Runo JR, Loyd JE. Primary pulmonary hypertension. *Lancet.* 2003;361:1533–1544.
5. Leung T, Manser E, Tan L, Lim L. A novel serine/threonine kinase binding the Ras-related RhoA GTPase which translocates the kinase to peripheral membranes. *J Biol Chem.* 1995;270:29051–29054.
6. Ishizaki T, Maekawa M, Fujisawa K, Okawa K, Iwamatsu A, Fujita A, Watanabe N, Saito Y, Kakizuka A, Morii N, Narumiya S. The small GTP-binding protein Rho binds to and activates a 160 kDa ser/thr protein kinase homologous to myotonic dystrophy kinase. *EMBO J.* 1996;15:1885–1893.
7. Amano M, Chihara K, Kimura K, Fukata Y, Nakamura N, Matsuura Y, Kaibuchi K. Formation of actin stress fibers and focal adhesions enhanced by Rho-kinase. *Science.* 1997;275:1308–1311.

8. Hall A. Rho GTPases and the actin cytoskeleton. *Science*. 1998;279: 509–514.
9. Narumiya S. The small GTPase Rho: cellular functions and signal transduction. *J Biochem (Tokyo)*. 1996;120:215–228.
10. Chihara S, Amano M, Nakamura N, Yano T, Shibata M, Tokui T, Ichikawa H, Ikebe R, Ikebe M, Kaibuchi K. Cytoskeletal rearrangements and transcriptional activation of c-fos serum response element by Rho-kinase. *J Biol Chem*. 1997;272:25121–25127.
11. Shimokawa H. Rho-kinase as a novel therapeutic in treatment of cardiovascular diseases. *J Cardiovasc Pharmacol*. 2002;39:319–327.
12. Mukai Y, Shimokawa H, Matoba T, Kandabashi T, Satoh S, Hiroki J, Kaibuchi K, Takeshita A. Involvement of Rho-kinase in hypertensive vascular disease: a novel therapeutic target in hypertension. *FASEB J*. 2002;15:1062–1064.
13. Shimokawa H, Seto M, Katsumata N, Amano M, Kozai T, Yamawaki T, Kuwata K, Kandabashi T, Egashira K, Ikegaki I, Asano T, Kaibuchi K, Takeshita A. Rho-kinase-mediated pathway induces enhanced myosin light chain phosphorylations in a swine model of coronary artery spasm. *Cardiovasc Res*. 1999;43:1029–1039.
14. Kandabashi T, Shimokawa H, Miyata K, Kunihiro I, Kawano Y, Fukata Y, Higo T, Egashira K, Takahashi S, Takahashi S, Kaibuchi K, Takeshita A. Inhibition of myosin phosphatase by upregulated Rho-kinase plays a key role for coronary artery spasm in a porcine model with interleukin-1β. *Circulation*. 2000;101:1319–1323.
15. Morishige K, Shimokawa H, Eto Y, Kandabashi T, Miyata K, Matsumoto Y, Hoshijima M, Kaibuchi K, Takeshita A. Adenovirus-mediated transfer of dominant-negative Rho-kinase induces a regression of coronary arteriosclerosis in pigs in vivo. *Arterioscler Thromb Vasc Biol*. 2001;21:548–554.
16. Masumoto A, Mohri M, Shimokawa H, Urakami L, Usui M, Takeshita A. Suppression of coronary artery spasm by a Rho-kinase inhibitor fasudil in patients with vasospastic angina. *Circulation*. 2002;105:1545–1547.
17. Miyata K, Shimokawa H, Kandabashi H, Higo T, Morishige K, Eto Y, Egashira K, Kaibuchi K, Takeshita A. Rho-kinase is involved in macrophage-mediated formation of coronary vascular lesions in pigs in vivo. *Arterioscler Thromb Vasc Biol*. 2000;20:2351–2358.
18. Cowan KN, Heilbut A, Humpl T, Lam C, Ito S, Rabinovitch M. Complete reversal of fatal pulmonary hypertension in rats by a serine elastase inhibitor. *Nat Med*. 2000;6:698–702.
19. Higashi M, Shimokawa H, Hattori T, Hiroki J, Mukai Y, Morikawa K, Ichiki T, Takahashi S, Takeshita A. Long-term inhibition of Rho-kinase suppresses angiotensin II–induced cardiovascular hypertrophy in rats in vivo: effect on endothelial NAD(P)H oxidase system. *Circ Res*. 2003;93: 767–775.
20. Cowan KN, Jones PL, Rabinovitch. Regression of hypertrophied rat pulmonary arteries in organ culture is associated with suppression of proteolytic activity, inhibition of tenascin-C, and smooth muscle cell apoptosis. *Circ Res*. 1999;84:1223–1233.
21. Matoba T, Shimokawa H, Nakashima M, Hirakawa Y, Mukai Y, Hirano K, Kanaide H, Takeshita A. Hydrogen peroxide is an endothelium-derived hyperpolarizing factor in mice. *J Clin Invest*. 2000;106:1521–1530.
22. Kondo T, Takeuchi K, Doi Y, Yonemura S, Nagata S, Tsukita S. ERM (ezrin/radixin/moesin)-based molecular mechanism of microvillar breakdown at an early stage of apoptosis. *J Cell Biol*. 1997;139:749–758.
23. Takemoto M, Sun J, Hiroki J, Shimokawa H, Liao JK. Rho-kinase mediates hypoxia-induced downregulation of endothelial nitric oxide synthase. *Circulation*. 2002;106:57–62.
24. Mitani Y, Mutlu A, Russell JC, Brindley DN, DeAlmeida J, Rabinovitch M. Dexfenfluramine protects against pulmonary hypertension in rats. *J Appl Physiol*. 2002;93:1770–1778.
25. Zhao YD, Campbell AI, Robb M, Ng D, Stewart DJ. Protective role of angiopoietin-1 in experimental pulmonary hypertension. *Circ Res*. 2003; 92:984–991.
26. Funakoshi Y, Ichiki T, Shimokawa H, Egashira K, Takeda K, Kaibuchi K, Takeya M, Yoshimura T, Takeshita A. Rho-kinase mediates angiotensin II -induced monocyte chemoattractant protein-1 expression in rat vascular smooth muscle cells. *Hypertension*. 2001;38:100–104.
27. Yamamoto Y, Ikegaki I, Sasaki Y, Uchida T. The protein kinase inhibitor fasudil protects against ischemic myocardial injury induced by endothelin-1 in the rabbit. *J Cardiovasc Pharmacol*. 2000;35:203–211.
28. Kanno S, Wu YJ, Lee PC, Billiar TR, Ho C. Angiotensin-converting enzyme inhibitor preserves p21 and endothelial nitric oxide synthase expression in monocrotaline-induced pulmonary arterial hypertension in rats. *Circulation*. 2001;104:945–950.
29. Channick RN, Simonneau G, Sitbon O, Robbins IM, Frost A, Tapson VF, Badesch DB, Roux S, Rainisio M, Bodin F, Rubin LJ. Effects of the dual endothelin-receptor antagonist bosentan in patients with pulmonary hypertension: a randomised placebo-controlled study. *Lancet*. 2001;358:1119–1123.
30. Ravinovitch M. Linking a serotonin transporter polymorphism to vascular smooth muscle proliferation in patients with primary pulmonary hypertension. *J Clin Invest*. 2001;108:1109–1111.
31. Hiroki J, Kandabashi T, Hattori T, Mukai Y, Kawamura N, Ichiki T, Shimokawa H. Inflammatory stimuli upregulate Rho-kinase in human coronary vascular smooth muscle cells: divergent effects of estrogen and nicotine. *Circulation*. 2002;106(suppl II):II-222. Abstract.
32. Eto M, Kozai T, Cosentino F, Joch H, Lüscher TF. Statin prevents tissue factor expression in human endothelial cells: role of Rho/Rho-kinase and Akt pathways. *Circulation*. 2002;105:1756–1759.
33. Nishimura T, Faul JL, Berry GJ, Vaszar LT, Qui D, Pear RG, Kao PN. Simvastatin attenuates smooth muscle neointimal proliferation and pulmonary hypertension in rats. *Am J Respir Crit Care Med*. 2002;166:1403–1408.
34. Nishimura T, Vaszar LT, Faul JL, Zhao G, Berry GJ, Shi L, Qiu D, Benson G, Pearl RG, Kao PN. Simvastatin rescues rats from fatal pulmonary hypertension by inducing apoptosis of neointimal smooth muscle cells. *Circulation*. 2003;108:1640–1645.
35. Girgis RE, Li D, Zhan X, Garcia JGN, Tuder RM, Hassoun PM, Johns RA. Attenuation of chronic hypoxic pulmonary hypertension by simvastatin. *Am J Physiol*. 2003;25:H938–H945.
36. Nagaoka T, Morio Y, Casanova N, Bauer N, Gebb S, McMurtry I, Oka M. Rho/Rho-kinase signaling mediates increased basal pulmonary vascular tone in chronically hypoxic rats. *Am J Physiol Lung Cell Mol Physiol*. September 5, 2003; 10.1152/ajplung.00050.2003. Available at: http://ajplung.physiology.org. Accessed December 7, 2003.
37. Matsumoto Y, Uwatoku T, Oi K, Abe K, Hattori T, Morishige K, Eto Y, Fukumoto Y, Nakamura K, Shibata Y, Matsuda T, Akira T, Shimokawa H. Long-term inhibition of Rho-kinase suppresses neointimal formation after stent implantation in porcine coronary arteries: involvement of multiple mechanisms. *Arterioscler Thromb Vasc Biol*. 2004;24:181–186. Published online before print October 30, 2003; 10.1161/01.ATV.0000105053.46994.5B.
38. Hattori T, Shimokawa H, Higashi M, Hiroki J, Mukai Y, Kaibuchi K, Takeshita A. Long-term treatment with a specific Rho-kinase inhibitor suppresses cardiac allograft vasculopathy in mice. *Circ Res*. 2004;94: 46–52. Published online before print November 13, 2003; 10.1161/01.RES.0000107196.21335.2B.
39. Sawada N, Itoh H, Ueyama K, Yamashita J, Doi K, Chun TH, Inoue M, Masatsugu K, Saito T, Fukunaga Y, Sakaguchi S, Arai H, Komeda M, Nakao K. Inhibition of Rho-associated kinase results in suppression of neointimal formation of balloon-injury arteries. *Circulation*. 2000;101:2030–2033.
40. Horwitz AR, Parsons JT. Cell migration: movin' on. *Science*. 1999;286: 1102–1103.
41. Ito K, Nakashima T, Murakami K, Murakami T. Altered function of pulmonary endothelium following monocrotaline-induced lung vascular injury in rats. *Br J Pharmacol*. 1988;94:1175–1183.
42. Tyler RC, Muramatsu M, Abman SH, Stelzner TJ, Rodman DM, Bloch KD, McMurtry IF. Variable expression of endothelial NO synthase in three forms of rat pulmonary hypertension. *Am J Physiol*. 1999;276:L297–L303.
43. Michelakis E, Tymchak W, Lien D, Webster L, Hashimoto K, Archer S. Oral sildenafil is an effective and specific pulmonary vasodilator in patients with pulmonary arterial hypertension. *Circulation*. 2002;105:2398–2403.
44. Robertson TP, Dipp M, Ward JP, Aaronson PI, Evans AM. Inhibition of sustained hypoxic vasoconstriction by Y-27632 in isolated intrapulmonary arteries and perfused lung of the rat. *Br J Pharmacol*. 2000;131:5–9.
45. Sauzeau V, Rolli-Derkinderen M, Lehoux S, Loirand G, Pacaud P. Sildenafil prevents change in RhoA expression induced by chronic hypoxia in rat pulmonary artery. *Circ Res*. 2003;93:630–637.
46. Wang Z, Jin N, Gangule S, Swartz DR, Li L, Rhoades RA. Rho-kinase activation is involved in hypoxia-induced pulmonary vasoconstriction. *Am J Respir Cell Mol Biol*. 2001;25:628–635.
47. Abe K, Uwatoku T, Oi K, Hizume T, Shimokawa H. Long-term inhibition of Rho-kinase ameliorates hypoxia-induced pulmonary hypertension *in* mice independent of endothelial NO synthase. *Circulation*. 2003; 108(suppl IV):IV-294. Abstract.
48. Nishimura T, Faul JL, Berry GJ, Veve I, Pearl RG, Kao PN. 40-*O*-(2-hydroxyethyl)-rapamycin attenuates pulmonary arterial hypertension and neointimal formation in rats. *Am J Respir Crit Care Med*. 2001;163:498–502.
49. Shimokawa H, Hiramori K, Iinuma H, Hosoda S, Kishida H, Osada H, Katagiri T, Yamauchi K, Minamino T, Nakashima M, Kato K. Anti-anginal effect of fasudil, a Rho-kinase inhibitor, in patients with stable effort angina: a multicenter study. *J Cardiovasc Pharmacol*. 2002;40:751–761.

PTEN and other tumor suppressor gene mutations as secondary genetic alterations in synovial sarcoma

TSUYOSHI SAITO[1], YOSHINAO ODA[1], KEN-ICHI KAWAGUCHI[1], TOMONARI TAKAHIRA[1], HIDETAKA YAMAMOTO[1], KAZUHIRO TANAKA[2], SHUICHI MATSUDA[2], AKIO SAKAMOTO[2], YUKIHIDE IWAMOTO[2] and MASAZUMI TSUNEYOSHI[1]

Departments of [1]Anatomic Pathology, and [2]Orthopaedic Surgery, Graduate School of Medical Sciences, Kyushu University, Fukuoka, Japan

Received September 12, 2003; Accepted November 12, 2003

Abstract. Synovial sarcomas (SS) consistently show a characteristic chromosomal translocation, t(X;18)(p11;q11), which usually leads to the formation of 2 chimeric fusion transcripts, SYT-SSX1 and -SSX2. A recent multi-institutional retrospective study revealed that the SYT-SSX fusion type emerged as the only independent significant factor for overall survival in cases of SS. The aims of this study were; i) to investigate the frequency of PTEN gene alteration, ii) to evaluate whether the mutation status in various tumor suppressor genes (TSG) is responsible for the clinical and histologic heterogeneity in SS. Forty-nine cases of SS were examined for the presence of PTEN gene mutation by polymerase chain reaction - single-strand conformation polymorphism followed by DNA direct sequencing. The obtained data was combined with those of previously reported TSG mutations such as p53, adenomatous polyposis coli, and E-cadherin genes. Follow-up was available for 44 patients, and survival analysis was performed according to the mutation status of these TSG. PTEN mutations were detected in 7 cases (14.3%), and all of these were monophasic tumors. More than half of the mutations detected were located in exon 9, which has been shown to play a less important role in PTEN functioning, and the PTEN mutation was not associated with patients' prognosis. Mutations in these TSG other than silent mutations were detected in 20 out of 49 cases (40.8%), although the mutation status in TSG was not associated with overall survival rate in patients with SS. Secondary genetic alterations in these TSG seem to have a less important prognostic impact on patients with SS.

Correspondence to: Dr Masazumi Tsuneyoshi, Department of Anatomic Pathology (Second Department of Pathology), Pathological Sciences, Graduate School of Medical Sciences, Kyushu University, Maidashi 3-1-1, Higashi-ku, Fukuoka 812-8582, Japan
E-mail: masazumi@surgpath.med.kyushu-u.ac.jp

Key words: PTEN, tumor suppressor genes, molecular target, prognosis, synovial sarcoma

Introduction

Synovial sarcomas consistently show a characteristic chromosomal translocation, t(X;18)(p11;q11), which usually represents either of 2 chimeric fusion transcripts, SYT-SSX1 or -SSX2 (1). In addition to the classical adverse prognostic factors such as advanced stage and tumor size, some molecular markers also have been described recently. The SYT-SSX2 fusion emerged as the only independent significant factor for better overall survival in patients with localized synovial sarcoma (2). This clinical difference may be attributed to the functional differences in transactivating potential between the fusion types of the SYT-SSX chimeric transcription factor (3,4).

During the progression of tumors, secondary genetic alterations may occur and provide an additional growth advantage to tumor cells, causing another source of clinical heterogeneity. In fact, clinical heterogeneity has also been described in cases of SS that cannot be explained only by SYT-SSX. These secondary molecular alterations involve tumor suppressor genes (TSG), including those regulating cell proliferation and cell adhesion, and some secondary genetic alterations have also been described in synovial sarcoma (5-9). In Ewing sarcoma/primitive neuroectodermal tumor (PNET) family tumor, the *INK4A* deletion was a negative prognostic factor in multivariate analysis as the most frequent secondary molecular genetic alterations (10). Nonetheless, the prognostic impact of these TSG alterations in SS remains unclear.

The tumor suppressor gene PTEN has been identified on chromosome 10q23.3 and is homozygously deleted in many human malignancies (11). Germ-line PTEN mutations have been detected in patients with autosomal dominant cancer predisposition syndromes (12,13). Somatic mutations and deletions of this gene have been reported in many types of sporadic tumors, including endometrial cancers, glioblastomas, prostate cancers, and melanomas (14-25). The PTEN gene encodes a phosphatidylinositol (PI) phosphatase, and the product is reported to induce apoptosis and G1 cell cycle arrest by antagonizing the PI 3'-kinase/Akt-mediated cell growth pathway (26,27). An aggressive phenotype in some types of tumors is reported to be associated with alterations of this gene (21). We recently reported that PTEN gene mutation

Table I. PTEN mutations in synovial sarcoma.

Case no.	Age/sex	Subtype	Position	Mutation	Prognosis
33	49/M	Fibrous	Exon 6 (codon 197)	AAG (Lys)→AAA (Lys)	Unknown
28	28/F	Fibrous	Exon 7 (codon 251)	Ins A (FS and stop at codon 252)	Alive (118 mos)
36	21/M	Fibrous	Exon 8 (codon 298)	CAA (Gln)→TAA (Stop)	DOD (28 mos)
21	11/M	Fibrous	Intron 4 to exon 5	accacag/TTGCA→atcacag/TTGCA	Alive (77 mos)
30	25/M	Fibrous	Exon 9 (codon 346)	TAC (Tyr)→CAC (His)	Alive (40 mos)
			Exon 9 (3'-UTR)	Del T; TGA/A(T)9ATCA→TGA/A(T)8ATCA	
3	47/F	Fibrous	Exon 9 (codon 348)	ACA (Thr)→ATA (Ile)	DOD (85 mos)
			Exon 9 (codon 367)	CCA (Pro)→CTA (Leu)	
32	30/F	Fibrous	Exon 9 (codon 355)	TCA (Ser)→TCG (Ser)	Unknown

UTR, untranslated region; FS, frameshift; stop, stop codon formation.

is a rare event in soft tissue sarcomas without specific balanced translocations such as malignant fibrous histiocytoma (MFH), leiomyosarcoma (LMS), and malignant peripheral nerve sheath tumor (MPNST), but 2 cases identified to have PTEN mutation were intra-abdominal LMS, providing a possible heterogeneity of molecular pathogenesis of LMS (28). These findings raise the possibility that the loss of PTEN function is also responsible for the clinical and histologic heterogeneity in SS.

The purpose of this study was first to investigate the frequency of PTEN gene alteration in SS. We also estimated the prognostic impact on the overall survival rate of the PTEN and other TSG we have previously investigated, such as p53, E-cadherin, adenomatous polyposis coli (APC) gene mutations as secondary genetic alterations in SS with specific balanced translocation (5,6,8).

Materials and methods

Materials and DNA preparation. In this study we used 49 cases of SS, most of which had been investigated in previous studies (5-8). Materials were fixed in a 10% formaldehyde solution and embedded in paraffin. Histological subtypes were comprised of 42 cases of monophasic, 6 cases of biphasic, and 1 case of poorly differentiated types. The biphasic type of SS was defined as those cases in which apparent glandular structures could be recognized. Clinical data for these cases were collected from the medical records. Survival data were available for 44 cases. Follow-up ranged from 1 to 278 months (mean: 66.7 months). Genomic DNA was purified from materials fixed in a 10% formaldehyde solution and embedded in paraffin, using standard proteinase K digestion and phenol/chloroform extraction.

Polymerase chain reaction-single strand conformation polymorphism (PCR-SSCP) and mutational analysis of the PTEN/MMAC1 gene. PCR-SSCP was performed for the PTEN gene from exon 5 to 9 using previously described pairs of primers (22,23). PCR was carried out in a Gene Amp PCR System 9600 (Perkin-Elmer, Foster City, CA, USA.) for 40 cycles after initial denaturing at 96°C for 5 min in a total volume of 20 μl of reaction mixture containing 50 ng of genomic DNA of each sample. Each cycle consisted of denaturation at 96°C for 1 min, at 58°C for 1 min, and at 72°C for 1 min. After the final cycle of amplification, the extension was continued for an additional 7 min at 72°C. Annealing temperatures were the same for each pair of primers. SSCP was performed using a gel containing 12.5% acrylamide (GenePhor™, Amersham Pharmacia Biotech, Uppsala, Sweden) and a DNA fragment analyzer (GenePhor) at 600 V, 25 mA, 15 W, and 5°C for 120 min, and then the DNA bands were visualized by a DNA Silver staining kit (GenePhor). The direct sequences were performed for samples with aberrantly migrating bands by SSCP as previously described (7). The sequence data were collected by ABI PRISM 310 Collection Software and were analyzed by Sequencing Analysis and Sequence Navigator Software (Perkin-Elmer). Furthermore, in order to rule out the possibility of single nucleotide polymorphisms or germ line mutation, genomic DNA was extracted from corresponding non-tumoral tissue in each case of SS with a PTEN mutation, and then direct sequences were performed.

Statistical analysis. The significance of mutations in the PTEN and other previously investigated TSG on the overall survival rate was estimated using the log-rank test (5,6,8). A $p<0.05$ was considered significant.

Results

PTEN gene mutation. The results are summarized in Table I and Fig. 1. We screened PTEN gene mutations from exon 5 to 9 in 49 cases of SS, and found 9 mutations in 7 (14.3%) of these specimens. Two cases had 2 mutations in this gene. There were 3 missense, 1 nonsense, and 2 silent mutations. In addition, in case 21, a C→T change between the intron 4 and exon 5 boundary was detected, which might have caused a splicing variant (Fig. 1A). A frame-shift mutation was also detected. In case 28, an insertion A at codon 251 was observed, which causes a frameshift followed by premature stop codon formation at codon 252 (Fig. 1B). Furthermore, a deletion of T at the 3'-untranslated region (UTR) was observed in case 30. All tumors with PTEN gene mutations were histologically monophasic fibrous tumors. All of these mutations could not be detected in the normal corresponding DNA (data not shown).

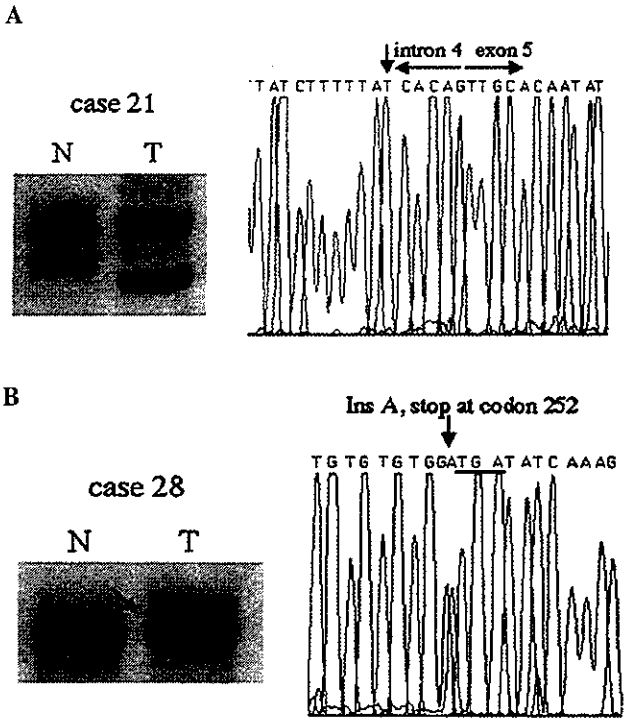

Figure 1. A, Results of PCR-SSCP (left) and direct sequencing (right) of the PTEN gene in case 21. Aberrantly migrating bands can be observed in only tumor-derived DNA (arrows). Direct sequencing of tumor-derived DNA shows a base change from C→T on the boundary between intron 4 and exon 5, which can cause a splicing variant (arrow). T, Tumor-derived DNA; N, corresponding normal tissue-derived DNA. B, Results of PCR-SSCP (left) and direct sequencing (right) of the PTEN gene in case 28. Aberrantly migrating bands can be observed in only tumor-derived DNA (arrows). Direct sequencing of tumor-derived DNA shows an insertion A at codon 251, which causes a frameshift followed by premature stop codon formation (TGA) at codon 252 (arrow).

Survival impact of PTEN and other tumor suppressor genes. We estimated the survival impact of PTEN gene mutation status, with silent mutations treated as mutation negative in our analyses. Fig. 2A shows the Kaplan-Meier overall survival curves for both groups of patients, that is, those with the PTEN mutant versus PTEN wild-type. Mutation of the PTEN gene was associated with a trend toward better survival during the first 5 years, though there was no statistically significant difference between the 2 groups (Fig. 2A, p=0.44). Recently it has been demonstrated that PTEN transcription is regulated by p53 through binding PTEN promoter (29). We previously reported on p53 mutation in cases of SS using almost the same group of patients (8). In the present study, we also evaluated the interaction between PTEN gene and p53 gene, because p53 mutations, which could cause the functional loss of this protein, also may affect the function of PTEN. In this series of 49 cases of SS samples, we observed a p53 mutation in 8 cases (16.3%), 6 of which harbored at least one missense or nonsense mutation. Fig. 2B shows the Kaplan-Meier overall survival curves for patients with the PTEN/p53 mutant versus those with PTEN/p53 wild-type. Patients of the PTEN/p53 mutant group showed a survival advantage over those in the PTEN/p53 wild-type group, although the difference was not statistically significant (Fig. 2B, p=0.13). Finally, we investigated the survival impact of PTEN/p53/E-cadherin/APC gene alterations (5,6,8). In this series, E-cadherin and

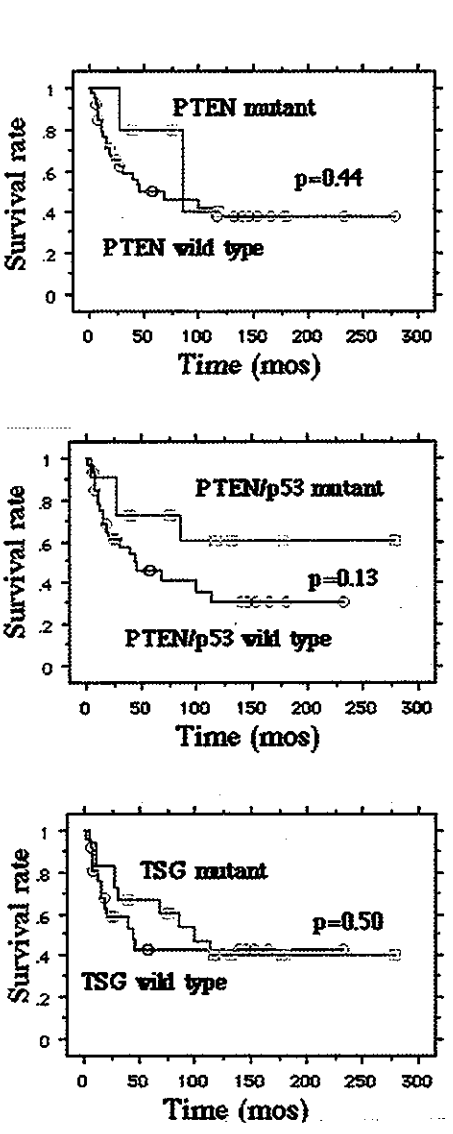

Figure 2. A, The Kaplan-Meier overall survival curves for both patients with the PTEN mutant and patients with PTEN wild-type. Mutation of the PTEN gene was associated with a trend toward better survival during at least the first 5 years, though there was no statistically significant difference between the 2 groups (p=0.44). B, The Kaplan-Meier overall survival curves for both patients with the PTEN/p53 mutant and patients with PTEN/p53 wild-type. The PTEN/p53 mutant group showed a survival advantage over the PTEN/p53 wild-type group, although the difference was not statistically significant (p=0.13). The label PTEN/p53 mutant implies that at least 1 of the PTEN/p53 genes is mutated. C, The Kaplan-Meier overall survival curves for both patients with TSG mutant and patients with TSG wild-type. However, mutation status of these TSG did not affect patients' prognosis (p=0.50). Cases with silent mutations were regarded as TSG wild-type in this analysis.

APC gene mutations except for silent ones were detected in 12 and 3 cases, respectively. Mutations of these TSG except for silent ones were detected in 20 out of 49 cases (40.8%); however, the mutation status of these TSG did not affect patients' prognosis (Fig. 2C, p=0.50).

Discussion

The region on chromosome 10q that harbors the PTEN gene and other tumor suppressor genes, such as the MXI1 gene (30), is known to be hemizygously deleted in many human

cancers, with a frequency reaching 60-80% in prostate cancers, endometrial cancers, and malignant glioblastomas (11,21,24,25,27). In tumors with hemizygous deletions at chromosome 10q23, PTEN gene mutations have been reported to occur at varying degrees of frequency. The PTEN mutation was reported to be a rare event in cases of chondrosarcoma, being present only in 1 of 40 samples of clinical specimens and cell lines (31). As far as its frequency in SCS, we recently reported that PTEN gene mutation is a rare event in soft tissue sarcomas without specific balanced translocations, but two LMS with PTEN mutation were of intra-abdominal origin, providing a possible heterogeneity of molecular pathogenesis of LMS (28). These findings raised the possibility that the loss of PTEN function accounts for the clinical and histologic heterogeneity in SS. Therefore, we examined the genetic alterations of PTEN from exon 1 to exon 4, because this region is described to be a mutation hot-spot (27). As a result, we have reported here that the PTEN gene mutations occur in SS with a frequency of 14.3%, higher rate than that of SCS.

According to Knudson's two-hit hypothesis (32), tumor suppressor gene function is lost as a result of independent inactivation events of both parental alleles. In this study, although the allele status of the tumors with PTEN mutations remains unclear, we observed dense mobility shift bands but a loss of or only faint normal bands in all 6 cases with these PTEN mutations other than silent ones, as shown in Fig. 1. These findings suggest that the PTEN gene is potentially inactivated in accordance with the 'two-hit hypothesis' in some cases of SS.

The prognostic significance of PTEN mutations has been reported in some types of carcinomas (15,16,21,22). It has been demonstrated that PTEN inactivation is a marker for an aggressive phenotype in glioblastoma, prostate carcinoma, and melanoma (17,18,21,25). In contrast, several studies have shown that PTEN mutation is associated with favorable prognosis in endometrial carcinoma (15,16,22). In this study, we observed no difference between the PTEN mutant group and PTEN wild-type group in the overall survival rate of patients with SS, although mutation of the PTEN gene was associated with a trend toward better survival at least during the first 5 years. It was demonstrated that the PTEN promoter contains a functional p53 binding site and that PTEN mRNA and protein levels increase in response to stimuli that result in p53 induction (29). Therefore, we also examined the possible inactivation of the PTEN via p53 mutation in SS and the impact on survival by using data from our previous study (8). We found that the PTEN/p53 mutant had a tendency toward favorable clinical outcome in SS, although the results were not statistically significant. These findings suggest that the PTEN-mediated apoptosis does not affect patients' survival and that the PTEN inactivation in SS is associated with rather favorable prognosis, as is demonstrated in endometrial carcinoma.

It is interesting to note the position of mutated exons of the PTEN gene in SS, as more than half of the mutations are in exon 9. According to the review of PTEN mutational spectra by Ali *et al* (27) the PTEN mutation in exon 9 is rare and has been reported in only a few cancers such as glioblastoma and breast cancer (19,20). The crystal structure of PTEN reported by Lee *et al* reveals that it contains a phosphatase domain and a C2 domain from exon 5 to 8 (33). In contrast, exon 9 seems to contain a less important domain, compared to exons 5-8, although functionally a deletion of T in the 3'-UTR found in case 30 may be associated with differences in transcript stability determined by the different 3' UTRs (33). It has been demonstrated that the presence of PTEN mutations located outside exons 5, 6, and 7 is an independent favorable prognostic factor in endometrial carcinomas (22). Therefore, it seems unlikely that most of the mutations detected in SS cause a complete functional loss of PTEN. The phenomenon of the rather favorable prognosis of patients with PTEN mutation in cases of SS might reflect these findings.

The prognostic impact of the SYT-SSX fusion gene has been suggested in synovial sarcoma (1,2). Recently, Ladanyi *et al* reported that the SYT-SSX fusion type was the single most significant prognostic factor by multivariate analysis in patients with localized disease (2). However, the clinical heterogeneity in cases of synovial sarcoma they studied makes it unlikely that the cause was attributed to only the SYT-SSX fusion gene (2). Therefore, we have examined mutations of the PTEN and other tumor suppressor genes to elucidate the survival impact of these genes as a secondary genetic alteration in synovial sarcoma (5,6,8). In Ewing sarcoma/primitive neuroectodermal tumor, which have been shown to have a specific fusion gene, it has been demonstrated that INK4A deletions occur as the most frequent secondary molecular genetic alteration, and such deletions are a strong negative factor for survival in multivariate analysis (10). We have examined various TSG alterations, including the PTEN gene mutations in this study, and 20 of 49 cases (40.8%) harbored at least one of these TSG alterations in synovial sarcoma. Nonetheless, the molecular alterations in TSG had no association with patients' overall survival rate, as shown in Fig. 2C. These findings suggest that these secondary genetic alterations in TSG have a less important prognostic impact in cases of SS, compared to the SYT-SSX fusion gene. However, these secondary genetic alterations in TSG might still be a target for future therapeutic strategies since these alterations might modify the progression of SS and explain the clinical heterogeneity in SS.

Finally, it is interesting to note that all cases with the PTEN mutation were monophasic tumors, although the number of biphasic tumors examined in this series is too small to state that PTEN does not play a role in biphasic SS. Some determinants of histological features or factors that might influence to the morphology of tumor cells in SS have been identified (1,2,4-7,34). PI(4,5)P2 locates at the cell membrane and is capable of binding to actin-binding-proteins, indicating that PI(4,5)P2 acts as mediator to bind cell membrane to actin-cytoskeleton (35). Therefore, PTEN has been considered to have an important role in maintaining cell shape, because PTEN has a function to dephosphorylate PIP3 to PI(4,5)P2. These findings suggest that loss of the PTEN function may be one of the determinants of histology, which works against the epithelial differentiation of tumor cells in SS.

In conclusion, we analyzed 49 cases of SS for the presence of PTEN gene mutation. PTEN mutations were detected in

7 cases (14.3%), and all of these were monophasic tumors. More than half of the mutations detected were located in exon 9, which has been shown to have a less important role in PTEN functioning. Although this study could not confirm the prognostic significance of the secondary change in TSG in SS, these secondary genetic alterations in TSG might still be a target for future therapeutic strategies since the downstream targets of the fusion gene might even be more important than the primary event.

Acknowledgements

This study was supported in part by a Grant-in-Aid for Scientific Research (C) (no. 15590304) from the Japan Society of the Promotion of Science, Tokyo, Japan. We thank KN International for revising the English used in this article.

References

1. Kawai A, Woodruff J, Healey JH, Brennan MF, Antonescu CR and Ladanyi M: SYT-SSX gene fusion as a determinant of morphology and prognosis in synovial sarcoma. N Engl J Med 338: 153-160, 1998.
2. Ladanyi M, Antonescu CR, Leung DH, Woodruff JM, Kawai A, Healey JH, Brennan MF, Bridge JA, Neff JR, Barr FG, Goldsmith JD, Brooks JS, Goldblum JR, Ali SZ, Shipley J, Cooper CS, Fisher C, Skytting B and Larsson O: Impact of *SYT-SSX* fusion type on the clinical behavior of synovial sarcoma: a multi-institutional retrospective study of 243 patients. Cancer Res 62: 135-140, 2002.
3. Dos Santos NR, De Bruijn DR and Geurts van Kessel A: Molecular mechanisms underlying human synovial sarcoma development. Genes Chromosomes Cancer 30: 1-14, 2001.
4. Ladanyi M: Fusions of the SYT and SSX genes in synovial sarcoma. Oncogene 20: 5755-5762, 2001.
5. Saito T, Oda Y, Sugimachi K, Kawaguchi K, Tamiya S, Tanaka K, Matsuda S, Sakamoto A, Iwamoto Y and Tsuneyoshi M: E-cadherin gene mutations frequently occur in synovial sarcoma as a determinant of histological features. Am J Pathol 159: 2117-2124, 2001.
6. Saito T, Oda Y, Sakamoto A, Kawaguchi K, Tanaka K, Matsuda S, Tamiya S, Iwamoto Y and Tsuneyoshi M: APC mutations in synovial sarcoma. J Pathol 196: 445-459, 2002.
7. Saito T, Oda Y, Sakamoto A, Tamiya S, Kinukawa N, Hayashi K, Iwamoto Y and tsuneyoshi M: Prognostic value of the preserved expression of the E-cadherin and catenin families of adhesion molecules and of ß-catenin mutations in synovial sarcoma. J Pathol 192: 342-350, 2000.
8. Oda Y, Sakamoto A, Saito T, Kawauchi S, Iwamoto Y and Tsuneyoshi M: Molecular abnormalities of p53, MDM2, and H-ras in synovial sarcoma. Mod Pathol 13: 994-1004, 2000.
9. Schneider-Stock R, Onnasch D, Haeckel C, Mellin W, Franke DS and Roessner A: Prognostic significance of p53 gene mutations and p53 protein expression in synovial sarcoma. Virchows Arch 435: 407-412, 1999.
10. Wei G, Antonescu CR, De Alava E, Leung D, Huvos AG, Meyers PA, Healey JH and Ladanyi M: Prognostic impact of INK4A deletion in Ewing sarcoma. Cancer 89: 793-799, 2000.
11. Steck PA, Pershouse MA, Jasser SA, Yung WK, Lin H, Ligon AH, Langford LA, Baumgard ML, Hattier T, Davis T, Frye C, Hu R, Swedlund B, Teng DH and Tavtigian SV: Identification of a candidate tumour suppressor gene, *MMAC1*, at chromosome 10q23.3 that is mutated in multiple advanced cancers. Nat Genet 15: 356-362, 1997.
12. Liaw D, Marsh DJ, Li J, Dahia PL, Wang SI, Zheng Z, Bose S, Call KM, Tsou HC, Peacocke M, Eng C and Parsons R: Germline mutations of the PTEN gene in Cowden disease, an inherited breast and thyroid cancer syndrome. Nat Genet 16: 64-67, 1997.
13. Marsh DJ, Dahia PL, Zheng Z, Liaw D, Parsons R, Gorlin RJ and Eng C: Germline mutations in PTEN are present in Bannayan-Zonana syndrome. Nat Genet 16: 333-334, 1997.
14. Van Gele M, Leonard JH, Van Roy N, Cook AL, De Paepe A and Speleman F: Frequent allelic loss at 10q23 but low incidence of PTEN mutations in Merkel cell carcinoma. Int J Cancer 92: 409-413, 2001.
15. Risinger JI, Hayes K, Maxwell GL, Carney ME, Dodge RK, Barrett JC and Berchuck A: PTEN mutation in endometrial cancers is associated with favorable clinical and pathologic characteristics. Clin Cancer Res 4: 3005-3010, 1998.
16. Maxwell GL, Risinger JI, Hayes KA, Alvarez AA, Dodge RK, Barrett JC and Berchuck A: Racial disparity in the frequency of PTEN mutations, but not microsatellite instability, in advanced endometrial cancers. Clin Cancer Res 6: 2999-3005, 2000.
17. Suzuki H, Freije D, Nusskern DR, Okami K, Cairns P, Sidransky D, Isaacs WB and Bova GS: Interfocal heterogeneity of PTEN/MMAC1 gene alterations in multiple metastatic prostate cancer tissues. Cancer Res 58: 204-209, 1998.
18. Celebi JT, Shendrik I, Silvers DN and Peacocke M: Identification of PTEN mutations in metastatic melanoma specimens. J Med Genet 37: 653-657, 2000.
19. Wang SI, Puc J, Li J, Bruce JN, Cairns P, Sidransky D and Parsons R: Somatic mutations of PTEN in glioblastoma multiforme. Cancer Res 57: 4183-4186, 1997.
20. Rhei E, Kang L, Bogomolniy F, Federici MG, Borgen PI and Boyd J: Mutation analysis of the putative tumor suppressor gene PTEN/MMAC1 in primary breast carcinomas. Cancer Res 57: 3657-3659, 1997.
21. Rasheed BK, Stenzel TT, McLendon RE, Parsons R, Friedman AH, Friedman HS and Bigner SH: PTEN gene mutations are seen in high-grade but not in low-grade gliomas. Cancer Res 57: 4187-4190, 1997.
22. Minaguchi T, Yoshikawa H, Oda K, Ishino T, Yasugi T, Onda T, Nakagawa S, Matsumoto K, Kawana K and Taketani Y: PTEN mutation located only outside exons 5, 6, and 7 is an independent predictor of favorable survival in endometrial carcinomas. Clin Cancer Res 7: 2636-2642, 2001.
23. Liu J, Babaian DC, Liebert M, Steck PA and Kagan J: Inactivation of MMAC1 in bladder transitional-cell carcinoma cell lines and specimens. Mol Carcinog 29: 143-150, 2000.
24. Risinger JI, Hayes AK, Berchuck A and Barrett JC: PTEN/MMAC1 mutations in endometrial cancers. Cancer Res 57: 4736-4738, 1997.
25. Cairns P, Okami K, Halachmi S, Halachmi N, Esteller M, Herman JG, Jen J, Isaacs WB, Bova GS, Sidransky D: Frequent inactivation of PTEN/MMAC1 in primary prostate cancer. Cancer Res 57: 4997-5000, 1997.
26. Di Cristofano A and Pandolfi PP: The multiple roles of PTEN in tumor suppression. Cell 100: 387-390, 2000.
27. Ali IU, Schriml LM, Dean M: Mutational spectra of PTEN/MMAC1 gene: a tumor suppressor with lipid phosphatase activity. J Natl Cancer Inst 91: 1922-1932, 1999.
28. Saito T, Oda Y, Kawaguchi K, Takahira T, Yamamoto H, Tamiya S, Tanaka K, Matsuda S, Sakamoto A, Iwamoto Y and Tsuneyoshi M: PTEN/MMAC1 gene mutation is a rare event in soft tissue sarcomas without specific balanced translocations. Int J Cancer 104: 175-178, 2003.
29. Stambolic V, MacPherson D, Sas D, Lin Y, Snow B, Jang Y, Benchimol S and Mak TW: Regulation of PTEN transcription by p53. Mol Cell 8: 317-325, 2001.
30. Wechsler DS, Shelly CA and Dang CV: Genomic organization of human MXI1, a putative tumor suppressor gene. Genomics 32: 466-470, 1996.
31. Lin C, Meitner PA and Terek RM: PTEN mutation is rare in chondrosarcoma. Diagn Mol Pathol 11: 22-26, 2002.
32. Knudson AG Jr, Hethcote HW and Brown BW: Mutation and childhood cancer: a probabilistic model for the incidence of retinoblastoma. Proc Natl Acad Sci USA 72: 5116-5120, 1975.
33. Lee JO, Yang H, Georgescu MM, Di Cristofano A, Maehama T, Shi Y, Dixon JE, Pandolfi P and Pavletich NP: Crystal structure of the PTEN tumor suppressor: implications for its phosphoinositide phosphatase activity and membrane association. Cell 99: 323-334, 1999.
34. Saito T, Oda Y, Sakamoto A, Tamiya S, Iwamoto Y and Tsuneyoshi M: Matrix metalloproteinase-2 expression correlates with morphological and immunohistochemical epithelial characteristics in synovial sarcoma. Histopathology 40: 279-285, 2002.
35. Vanhaesebroeck B, Leevers SJ, Ahmadi K, Timms J, Katso R, Driscoll PC, Woscholski R, Parker PJ and Waterfield MD: Synthesis and function of 3-phosphorylated inositol lipids. Annu Rev Biochem 70: 535-602, 2001.

c-kit and PDGFRA Mutations in Extragastrointestinal Stromal Tumor (Gastrointestinal Stromal Tumor of the Soft Tissue)

Hidetaka Yamamoto, MD, Yoshinao Oda, MD,* Ken-ichi Kawaguchi, MD,* Norimoto Nakamura, MD,* Tomonari Takahira, MD,* Sadafumi Tamiya, MD,* Tsuyoshi Saito, MD,*§ Yumi Oshiro, MD,† Masayuki Ohta, MD,‡ Takashi Yao, MD,* and Masazumi Tsuneyoshi, MD**

Abstract: Extragastrointestinal stromal tumor (EGIST) is a unique tumor that occurs outside the gastrointestinal tract. EGIST shows a c-kit expression and histologic appearance similar to those of gastrointestinal stromal tumor (GIST). Most GISTs have gain-of-functional mutation of the c-kit gene, and some have mutation of the platelet-derived growth factor receptor-alpha (PDGFRA) gene. However, the frequency of mutation of those genes in EGISTs remains unclear. We examined the clinicopathologic features, prognostic factors, and c-kit and PDGFRA mutation in 39 cases of EGIST. Tumors with high mitotic counts (≥5/50 high power fields) or a high Ki-67 labeling index (≥10%) were significantly correlated with worse prognoses. The c-kit mutation was found in the juxtamembrane domain (exon 11) and the extracellular domain (exon 9) in 12 of 29 cases (41.4%) and 2 of 29 cases (6.9%), respectively. The PDGFRA gene mutation was found at the juxtamembrane domain (exon 12) and the tyrosine kinase domain (exon 18) in one case each. The pattern of kit and PDGFRA mutation in EGIST was essentially similar to that in GIST. Our results suggest that the c-kit and PDGFRA mutations play an important role in the tumorigenesis of EGIST. High mitotic counts and a high Ki-67 labeling index may be useful for predicting the aggressive biologic behavior in EGIST. Furthermore, STI-571, targeting c-kit and PDGFR tyrosine kinase, seems to be a possible therapeutic strategy for EGISTs, especially advanced cases.

Key Words: extragastrointestinal stromal tumor, soft tissue, gastrointestinal stromal tumor, c-kit, PDGFRA, STI-571

(*Am J Surg Pathol* 2004;28:479–488)

From the *Department of Anatomic Pathology, Graduate School of Medical Sciences, Kyushu University, Fukuoka, Japan; Departments of †Pathology and ‡Surgery, Matsuyama Red Cross Hospital, Matsuyama, Japan; and §Department of Pathology, Memorial Sloan-Kettering Cancer Center, New York, NY.

This work was supported in part by 2003 Grant-in-Aid for Scientific Research (C) (no. 15590304) from the Japan Society of the Promotion of Science.

Reprints: Masazumi Tsuneyoshi, MD, Department of Anatomic Pathology, Pathological Sciences, Graduate School of Medical Sciences, Kyushu University, 3-1-1 Maidashi, Higashi-ku, Fukuoka, 812-8582, Japan (e-mail: masazumi@surgpath.med.kyushu-u.ac.jp).

Gastrointestinal stromal tumor (GIST) is the most common mesenchymal tumor of the gastrointestinal tract.[8,21] GIST is typically characterized by immunohistochemical expression of c-kit. The interstitial cell of Cajal also expresses c-kit and CD34.[11,28] Therefore, GIST is considered to show differentiation along the lines of interstitial cell of Cajal. Since Hirota et al first described the c-kit gene mutation in GIST,[11] several studies have revealed various types of c-kit oncogene mutations, including exon 11 encoding the juxtamembrane domain, exon 9 encoding the extracellular domain, and exons 13 and 17 encoding the tyrosine kinase domain.[3,7,12,16–18,23,26,27,30,31,34] Moreover, recent studies have described the mutations of PDGFRA at the juxtamembrane domain (exon 12) and tyrosine kinase domain (exon 18) in some populations of GIST.[9,10] In the earlier literature, GIST was classified as a smooth muscle tumor variously termed leiomyoma, epithelioid leiomyoma, leiomyoblastoma, leiomyosarcoma, epithelioid leiomyosarcoma, or malignant leiomyoblastoma. GIST of the digestive tract is now considered to be the distinctive entity, distinguished from leiomyoma, leiomyosarcoma, schwannoma, and other mesenchymal tumors.[20] Recently, Miettinen et al have reported c-kit positive tumors primarily in the omentum and mesentery.[22] Reith et al also have reported this kind of tumor, named extragastrointestinal stromal tumor (EGIST).[25] Furthermore, Sakurai et al have described a c-kit gene mutation at exon 11 in 5 cases of GISTs primarily in the omentum.[29] However, the frequency of c-kit and PDGFRA mutations, or the clinicopathologic importance of such mutations in a large series of EGISTs, is still poorly understood.

STI-571 (imatinib mesylate, [Gleevec]; Novartis Pharmaceuticals Corp, East Hanover, NL) is an anti-tyrosine kinase drug that was originally developed for bcr-abl in chronic myeloid leukemia.[6] Recent studies have revealed the anti-tumor effect of STI-571 in GIST.[4,14,32,33] In this study, we aimed to characterize the clinicopathologic features in a large series of EGISTs, and then elucidated the frequency of kit and PDGFRA abnormalities and their clinicopathologic importance for the targeted therapeutic strategy by STI-571.

MATERIALS AND METHODS

Case Materials

We reviewed leiomyomas, leiomyoblastomas, leiomyosarcomas, and other spindle cell tumors of the abdominal cavity, retroperitoneum, and pelvic cavity that were stored in the files of our department. Leiomyosarcomas were diagnosed as tumors showing histologically recognizable smooth muscle differentiation as shown by interlacing fascicles of spindle cells with eosinophilic cytoplasm and blunt-ended nuclei. All leiomyosarcomas were positive for smooth muscle actin, sometimes for desmin, and entirely negative for c-kit. We defined EGISTs as tumors fulfilling the following characteristics: 1) tumors that originate from the soft tissues of the abdominal cavity, retroperitoneum, and pelvic cavity, but display no connection to the wall of the gastrointestinal tract and the pelvic organs; 2) tumors showing histologic resemblance to homologous GIST; and 3) tumors with c-kit immunopositivity. In this study, the majority of EGISTs were diffusely and strongly positive for c-kit. Six cases with weak c-kit positivity were included in this study because they showed weak but diffuse immunoreactivity for c-kit, diffuse expression of CD34, and similar histologic features to those of other EIGSTs with strong immunoreactivity for c-kit.

Finally, 39 cases of EGIST were obtained. Each EGIST was evaluated for clinicopathologic and histologic features, including cell type (epithelioid or spindle), cellularity (low, moderate, or high), mitoses, and the presence of necrosis and hemorrhage. Mitoses were counted and summed from 50 high power fields (HPF).

Immunohistochemistry

Formalin-fixed paraffin-embedded samples were used for the immunohistochemical examination. Immunohistochemical staining was performed using the following primary antibodies: c-kit (polyclonal c-19, dilution; 1/200, Santa Cruz Biochemistry, CA.), CD34 (QB-end-10, dilution; 1/50, Novocastra, Newcastle, UK), alpha-smooth muscle actin (1A4, dilution; 1/5000, Sigma BioSciences, St. Louis, MO), muscle-specific actin (HHF35, dilution; 1/200, Biomedia, Foster City, CA), desmin (D33, dilution 1/100, DAKO, Carpinteria, CA), S-100 (polyclonal, dilution; 1/400, DAKO), and Ki-67 (MIB-1, dilution 1/100, DAKO). The subsequent development of antibody-bridge labeling was performed by the streptavidin-biotin-peroxidase method (Histofine SAB-PO Kit, Nichirei, Tokyo, Japan) with hematoxylin counterstaining.

Polymerase Chain Reaction Single-Strand Conformation Polymorphism (PCR-SSCP) for c-kit and PDGFRA

Mutations of exons 9, 11, 13, and 17 of the c-kit gene and those of exons 12 and 18 of the PDGFRA gene were examined in 29 cases of EGIST, according to the previously described PCR-SSCP methods.[35] Ten randomly selected cases of leiomyosarcomas were examined together. Genomic DNA was extracted from paraffin-embedded tissue by using standard proteinase K digestion and phenol/chloroform extraction. The DNA sequences for each exon were amplified for the first PCR with each primer for 40 cycles (94°C for 1 minute, 52–56°C for 1 minute, and 72°C for 1 minute) by using a thermal cycler (T Gradient, Biometra, Goettingen, Germany.). The annealing temperature and sequences of each primer are summarized in Table 1. The PCR products were electrophoresed through 2.0% agarose gel with ethidium bromide to confirm the correct amplification. The reamplified products were diluted 1:1 in loading buffer (94% formamide, 10 mg bromphenol blue, 0.05% xylene cyanol), denatured by heating at 98°C for 3 minutes, and snap frozen on ice, then loaded onto 12.5% polyacrylamide gel. Electrophoresis was carried out for 90 minutes at a constant power of 600 V using an electrophoretic apparatus (GenePhor System, Amersham Pharmacia Biotech, Tokyo, Japan) under the three different temperature conditions. After electrophoresis, the gels were stained using a DNA silver staining kit (Hoefer Automated Gel Stainer, Amersham Pharmacia Biotech). The samples showing abnormal migration bands by PCR-SSCP were reamplified for 25 cycles under the same conditions. The amplified products were then purified by centrifugal filter devices of Microcon (Millipore, Bedford, MA). After the purification, a direct sequencing was carried out by the dideoxy chain termination method using a Perkin Elmer ABI Prism 310 sequence analyzer (Applied Biosystems, Foster City, CA). If the sample did not show the abnormal migration bands in SSCP, direct sequencing was carried out.

Statistical Analysis

The correlation between the presence of mutation and the clinicopathologic parameters was analyzed by Fisher exact test and Student's *t* test. We analyzed disease-specific survival and disease-free survival. The end points included any relapse (local recurrence and/or distant metastasis) of EGIST for the analysis of disease-free survival and death from EGIST for the analysis of tumor-specific survival. Univariate analyses of both survivals were performed by the Kaplan-Meier method with a log-rank test.

RESULTS

Clinical Findings

The clinicopathologic findings of EGIST are summarized in Table 2. The 39 patients comprised 15 men and 24 women, ranging in age from 30 to 88 years (mean, 59 years). The tumors were located in the abdominal cavity (11 cases), omentum (3 cases), mesentery (3 cases), retroperitoneum (17 cases), and pelvic cavity (5 cases). Of 11 abdominal cases, 2 cases (case nos. 21 and 38) showed omental tumors with peri-

TABLE 1. Primer Sequences and Annealing Temperature for PCR

Exon	Primer Sequence	Annealing (°C)
c-kit		
9F	5′-TTT GGA AAG CTA GTG GTT CA-3′	52
9R	5′-ATG GTA GAC AGA GCC TAA AC-3′	
11F	5′-CTA TTT TTC CCT TTC TCC CC-3′	54
11R	5′-TAC CCA AAA AGG TGA CAT GG-3′	
13F	5′-GCT TGA CAT CAG TTT GCC AG-3′	56
13R	5′-AAA GGC AGC TTG GAC ACG GCT TTA-3′	
17F	5′-TTT CTC CTC CAA CCT AAT AG-3′	56
17R	5′-CCT TTG CAG GAC TGT CAA GC-3′	
PDGFRA		
12-1F	5′-CCA GTT ACC TGT CCT GGT CAT-3′	53
12-1R	5′-TGG AAA CTC CCA TCT TGA GTC-3′	
12-2F	5′-AAA TTC GCT GGA GGG TCA TT-3′	53
12-2R	5′-GGA GGT TAC CCC ATG GAA CT-3′	
18F	5′-AGT GTG TCC ACC GTG ATC TG-3′	53
18R	5′-GTG TGG GAA GTG TGG ACG TA-3′	

toneal dissemination, 1 case (case no. 4) showed a predominantly omental tumor with invasion to the mesocolon, 1 case (case no. 11) showed an omental tumor with invasion to the abdominal wall, 2 cases (case nos. 31 and 35) showed tumors located between the mesocolon and retroperitoneum, and 1 tumor (case no. 39) was located between the transverse colon and duodenum. As for the remaining abdominal tumors (case nos. 10, 18, and 29), further details of their origin were not available, but they did not display any definite connection to the gastrointestinal wall proper. Of the 5 pelvic tumors, 2 cases (case nos. 9 and 24) were located between the rectum and urinary bladder, 2 cases (case nos. 1 and 30) between the rectum and sacrum, and the other (case no. 36) at the right side of the uterus. Surgical excision was the primary treatment of all of the cases.

Follow-up information was available for 33 patients, and the follow-up period ranged from 5 to 192 months (median, 43 months). Fourteen patients (42.4%) were alive without any evidence of disease after the initial operation. Three patients (9.1%) were alive with a recurrent tumor. Distant metastasis was seen in 8 patients (24.2%), including liver metastasis (3 cases), lung metastasis (2 cases), both liver and lung metastasis (2 cases), and bone metastasis (1 case). Sixteen patients (48.5%) had died of the tumor. The cause of death was related to EGIST in all patients who died. The estimated 5-year tumor-specific and recurrence-free survival rate was 52.5% and 42.9%, respectively.

Pathologic Findings

The tumors ranged from 3 to 35 cm in size (mean, 13.5 cm). Grossly, most tumors presented as circumscribed or lobulated firm masses. Cystic change was recognized in several cases; in particular, 2 cases were present as a huge cystic mass. Histologically, 21 cases (54%) were predominantly of the spindle cell type and 18 (46%) were of the epithelioid type. The EGISTs of the spindle cell type consisted of short or ill-developed fascicles of spindled cells (Fig. 1A). These cells usually had short plump nuclei; these features are distinct from those of conventional leiomyosarcoma characterized by well-developed fascicles of spindle cells with blunt-ended nuclei and eosinophilic fibrillary cytoplasms. The EGISTs of the epithelioid cell type consisted of a sheet of rounded to polygonal cells, showing the features of benign or malignant leiomyoblastoma (Fig. 1B). Mild nuclear pleomorphism was observed in 13 cases (Fig. 1C, D). Some cases showed cytoplasmic vacuolization, resulting in signet-ring cell formation. Skenoid fibers were not observed in any cases. Mitotic counts varied from 0 to 100 per 50 HPF. Immunohistochemically, 33 tumors were strongly and diffusely positive for c-kit (Fig. 1E). Six cases showed weak but diffuse staining for c-kit. CD34 was positive in 24 (62%) cases. Alpha-smooth muscle actin, desmin, and S-100 protein were positive in 11 (31%), 2 (5%), and 2 cases (5%), respectively.

c-kit Mutation

Of 29 cases of EGIST available for molecular study, 12 (41.4%) showed the c-kit mutations at exon 11. Deletions ranging from 6 to 60 bp in exon 11 were found in 7 cases, and point mutations were found in 5 cases (Fig. 2). Two cases (6.9%) showed a mutation at exon 9, which was a 6-bp (GCCTAT) insertion at codon 504, resulting in duplication of Ala and Tyr (Fig. 3). None of the EGISTs had a mutation in

TABLE 2. Clinicopathologic Findings in 39 Cases of EGIST

Case No.	Age (yr)	Gender	Size (cm)	Site	Cell Type	Cellularity	Nuclear Pleomorphism
1	64	M	11	Pelvic cavity	Epithelioid	Moderate	+
2	80	F	15	Retroperitoneum	Spindle	Moderate	−
3	84	F	25	Mesentery	Epithelioid	Moderate	−
4	52	M	30	Abdominal cavity	Epithelioid	Moderate	+
5	46	F	7	Retroperitoneum	Epithelioid	High	−
6	69	M	18	Retroperitoneum	Spindle	High	+
7	64	F	4	Mesentery	Epithelioid	Moderate	−
8	62	F	11	Omentum	Epithelioid	Moderate	−
9	58	M	22	Pelvic cavity	Spindle	Moderae	−
10	54	M	15	Abdominal cavity	Epithelioid	Moderate	−
11	38	M	6	Abdominal cavity	Epithelioid	High	−
12	68	F	15	Retroperitoneum	Spindle	High	+
13	45	F	10	Retroperitoneum	Spindle	High	−
14	63	M	6	Retroperitoneum	Spindle	Moderate	−
15	54	M	15	Omentum	Epithelioid	Moderate	+
16	45	M	3	Retroperitoneum	Epithelioid	Moderate	−
17	50	F	14	Retroperitoneum	Spindle	High	−
18	45	F	25	Abdominal cavity	Epithelioid	High	−
19	49	F	17	Omentum	Epithelioid	Moderate	−
20	30	F	14	Retroperitoneum	Epithelioid	Low	−
21	80	M	10	Abdominal cavity	Epithelioid	Moderate	+
22	67	F	10	Retroperitoneum	Spindle	Moderate	+
23	56	F	12	Retroperitoneum	Spindle	High	+
24	88	M	15	Pelvic cavity	Epithelioid	Moderate	−
25	48	F	11	Retroperitoneum	Spindle	High	−
26	52	F	10	Retroperitoneum	Spindle	High	+
27	54	M	35	Retroperitoneum	Spindle	High	−
28	57	F	9	Retroperitoneum	Spindle	Moderate	−
29	62	F	5	Abdominal cavity	Spindle	High	−
30	65	F	8	Pelvic cavity	Spindle	High	−
31	55	M	15	Abdominal cavity	Spindle	High	−
32	54	M	15	Abdominal cavity	Spindle	High	+
33	74	F	14	Retroperitoneum	Spindle	Moderate	+
34	75	F	8	Retroperitoneum	Spindle	Moderate	+
35	79	F	10	Abdominal cavity	Spindle	Moderate	−
36	56	F	15	Pelvic cavity	Spindle	Moderate	−
37	54	F	16	Mesentery	Epithelioid	High	−
38	56	M	10	Abdominal cavity	Epithelioid	Moderate	+
39	63	F	15	Abdominal cavity	Epithelioid	Moderate	−

exons 13 or 17. In total, 14 of 29 (48.2%) cases of EGISTs had c-kit gene mutations. None of the 10 leiomyosarcomas had the kit mutation.

PDGFRA Mutation

The mutation of PDGFRA exon 12 was found in 1 case (case no. 3), showing GTC to GAC transition at codon 561 (V561D) (Fig. 4). One case (case no. 19) had a mutation at exon 18 with a 12-bp deletion of codon 842 to 845 (Del DIMH) (Fig. 4). In total, 2 of 29 (6.9%) EGISTs, or 2 of 15 (13.3%) kit-wild EGISTs, had PDGFRA mutations. Two cases with PDGFRA mutation had epithelioid morphology, a large tumor size (25 cm or 17 cm), low mitotic activity, and a low Ki-67 labeling index. One case with the exon 12 mutation (case no. 3)

TABLE 2. (Continued)

Case No.	Mitosis (/50 HPF)	Ki-67 LI	c-kit Mutation	PDGFRA Mutation	Local Recurrence (mo)	Metastasis (mo)	Final (mo)	Follow-up
1	4	10.8	–	–	+, 9	Lung, 7	AWD	22
2	9	3.9	–	–	–	–	NED	9
3	4	3.3	–	Exon 12	+, 5	–	DOD	5
4	4	2.3	–	–	–	–	NED	60
5	1	2.3	Exon 11	–	–	–	NED	86
6	12	17.2	–	–	+, 10	–	DOD	37
7	4	1	Exon 11	–	–	–	NED	192
8	3	1.2	–	–	–	–	NED	6
9	4	0.5	–	–	–	–	NED	126
10	5	0.5	–	–	–	–	NED	161
11	2	2.3	ND	ND	+, 5	–	DOD	5
12	5	3.2	ND	ND	+, 101	–	DOD	136
13	19	10	–	–	–	Lung, 24	DOD	50
14	4	4.1	Exon 11	–	+, 79	–	DOD	96
15	3	1	ND	ND	–	–	NED	62
16	1	2	Exon 11	–	–	–	NED	86
17	10	1	–	–	+, 52	Liver, 44	DOD	68
18	100	12.7	–	–	–	Spine, at present	DOD	13
19	1	2	–	Exon 18	–	–	NED	48
20	9	1.8	Exon 11	–	+, 10	–	DOD	21
21	17	6.6	Exon 9	–	+, 36	Liver, 55	AWD	55
22	20	33.9	Exon 11	–	–	Liver, 6	AWD	6
23	20	12.1	ND	ND	–	Liver, lung, 46	DOD	48
24	5	7	Exon 11	–	–	–	NED	13
25	50	1	Exon 11	–	+, 10	–	DOD	28
26	25	11.5	–	–	+, 54	Liver, lung, 54	DOD	60
27	0	2	–	–	–	–	NED	94
28	5	4.2	ND	ND	+, 9	–	DOD	9
29	25	7.5	–	–	–	–	NED	6
30	1	1	Exon 11	–	–	–	NED	175
31	15	8	Exon 11	–	+, 10	–	DOD	22
32	28	11.7	Exon 11	–	+, 10	–	DOD	21
33	4	1.9	ND	ND	+, 9	–	DOD	24
34	10	2.7	ND	ND	NA	NA	NA	
35	4	4	Exon 9	–	NA	NA	NA	
36	3	NA	ND	ND	NA	NA	NA	
37	24	8.1	ND	ND	NA	NA	NA	
38	8	NA	Exon 11	–	NA	NA	NA	
39	100	12.3	ND	ND	NA	NA	NA	

ND, not done; NA, not available; NED, no evidence of disease; AND, alive with disease; DOD, die of disease; LI, labeling index.

was malignant with short survival, whereas the other case with the exon 18 mutation (case no. 19) was free of recurrence for 4 years. The PDGFRA mutation was not found either in kit-mutant EGISTs or in leiomyosarcomas.

Statistical Analysis for Prognosis

Follow-up information was available for 33 patients, of which 27 were available for analysis of the c-kit gene and PDGFRA gene mutation. The tumors with the c-kit mutation

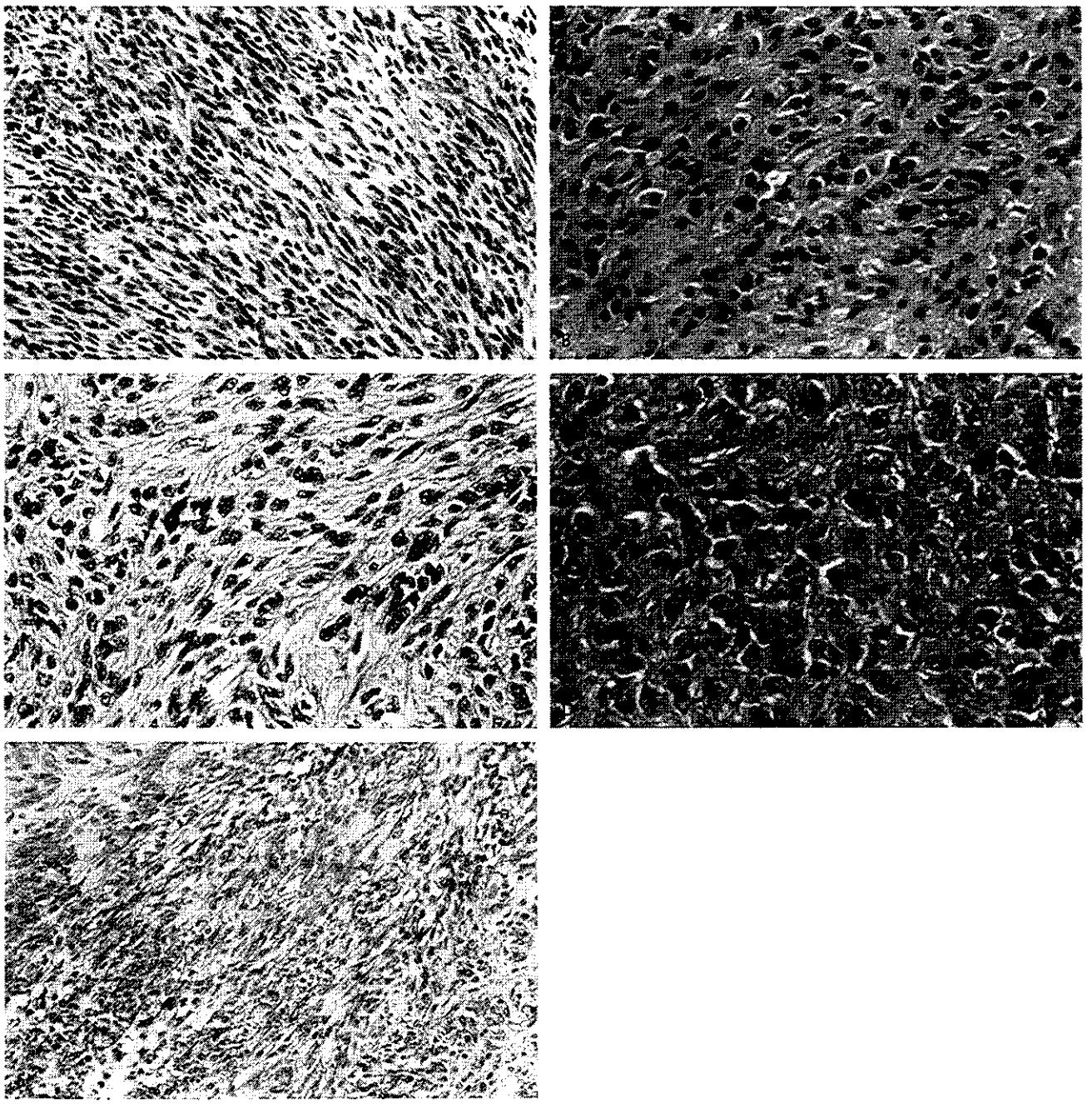

FIGURE 1. Histologic appearance of EGIST. **A:** Spindle cell type. Spindle tumor cells are arranged in fascicles with palisading pattern. **B:** Epithelioid cell type. Tumor cells with rounded nuclei are arranged in sheets. **C:** Spindle cell type with cellular atypia. Nuclear enlargement and irregularity are noted. **D:** Epithelioid cell type with cellular atypia. Nuclear enlargement and irregularity are noted. **E:** c-kit expression in EGIST.

were smaller in size than those without the mutation (P = 0.008). No other clinicopathologic factors correlated with the c-kit mutation in the 27 cases (Table 3). Even when moderate and high cellularity were combined, the cellularity (low vs. moderate, high) was not correlated with the presence of the c-kit mutation. The presence of the c-kit mutation was not correlated with either disease-specific survival or disease-free survival (P = 0.86 and P = 0.90, respectively). There was no significant correlation between the presence of gene mutation in either c-kit or PDGFRA and any clinicopathologic factors,

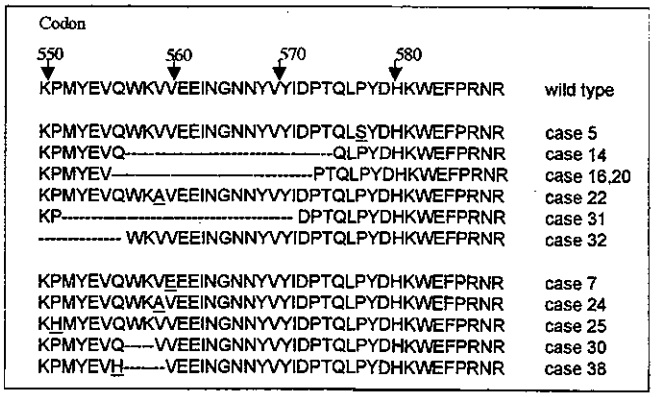

FIGURE 2. c-kit mutation at exon 11 and predicted amino acid sequence. -----, deletion. Point mutation is underlined.

including the prognosis. In 33 cases, a high mitotic rate (≥5/50 HPF) was significantly associated with both shorter disease-specific survival ($P = 0.015$) and shorter disease-free survival ($P = 0.014$) (Fig. 5). A high Ki-67 labeling index (≥10% HPF) also had significantly shorter disease-specific survival and shorter disease-free survival than those with a low index (<10%) ($P = 0.025$ and $P = 0.024$, respectively) (Fig. 5). We defined three categories on the basis of a combination of the mitotic rate and MIB-1 labeling index: the high-risk group (≥5/50 HPF with ≥10% Ki-67), the intermediate-risk group (≥5/50 HPF with <10% Ki-67, or, <5/50 HPF with ≥10% Ki-67), and the low-risk group (<5/50 HPF with <10% Ki-67).

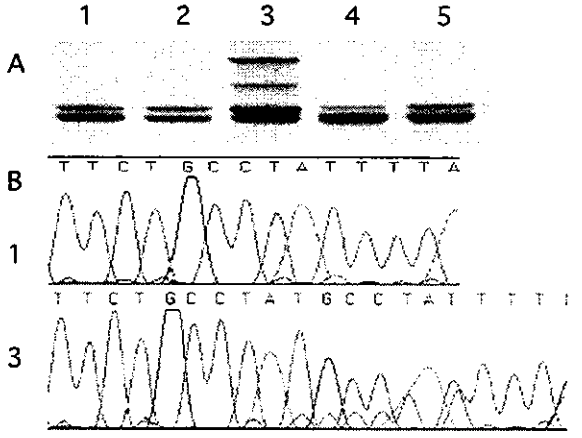

FIGURE 3. c-kit mutation at exon 9. **A:** The result of SSCP. Lane 3 (case no. 21) shows abnormally migrated bands corresponding to a 6-bp insertion. Lane 1, normal tissue (wild type); lane 2, EGIST, case no. 20 (exon 11 mutation-positive); lane 3, EGIST, case no. 21 (exon 9 mutation-positive); lane 4, case no. 1 (kit mutation-negative); lane 5, leiomyosarcoma. **B:** The results of DNA sequencing. The case in the lane 3 has a 6-bp (GCCTAT) insertion at codon 504. The sequence of lane 1 represents wild type of exon 9.

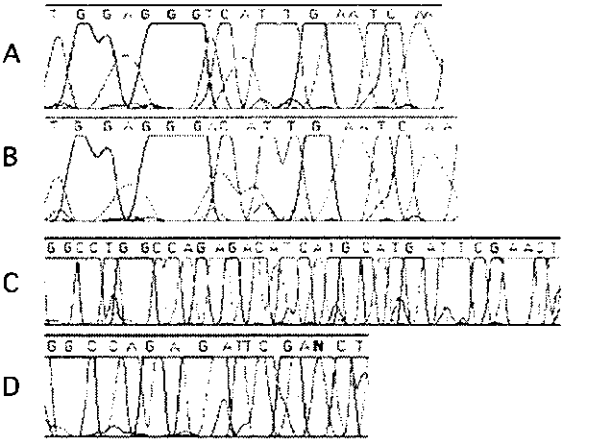

FIGURE 4. PDGFRA mutation. **A:** Wild type of exon 12. **B:** GTC to GAC transition at codon 561 (V561D) in exon 12 (case no. 3). **C:** Wild type of exon 18. **D:** A 12-bp deletion of codon 842 to 845 (Del DIMH) in exon 18 (case no. 19).

Based on the above grading system, 7 cases were classified as high risk, 12 as intermediate risk, and 14 as low risk. The risk-grade was significantly associated with disease-specific survival and disease-free survival ($P = 0.018$ and $P = 0.006$, respectively). None of the other factors, including tumor size, site, cellularity, nuclear pleomorphism, and cell type, correlated with both types of survival.

DISCUSSION

In the current study, we found the frequent c-kit expression and gene mutations in EGIST. Moreover, to the best of our knowledge, this is the first report of PDGFRA mutation in EGIST. Histologically, EGISTs had an identical appearance to GISTs that were located in the gastrointestinal tract proper. In addition, conventional leiomyosarcomas lacked c-kit expression and c-kit gene mutation in our previous and current studies, which are in accordance with the results reported by other laboratories.[13,15,17] Those data suggest that EGIST is the distinctive entity, distinguished from leiomyosarcoma. In the current series of EGISTs, the c-kit mutations were found to have the point mutation and deletion at exon 11 (juxtamembrane domain) in 12 of 29 cases (41.4%), and the identical tandem duplication of Ala and Tyr at codon 504 of exon 9 (extracellular domain) in 2 of 29 cases (6.9%), but not in the kinase domain (exons 13 and 17). The pattern of c-kit mutation found in our EGISTs was similar to that found in GISTs. These mutations have been demonstrated to result in ligand-independent phosphorylation and activation of the c-kit tyrosine kinase in GISTs.[11,12] Therefore, it is suggested that c-kit mutations play an important role in the tumorigenesis of EGISTs. Several large studies in which more than three regions of the c-kit gene were investigated revealed the mutations in approximately 40% to 90% of GISTs, including the mutations in exon 11

TABLE 3. Clinicopathologic Findings of 27 Cases of EGISTs With and Without c-kit Mutation

Variable	c-kit Mutation Positive (n = 12)	c-kit Mutation Negative (n = 15)	*P*
Age (yr)	58.8 ± 16	58.7 ± 12	NS
Gender			
M	6	6	NS
F	6	9	
Site			
Abdomen	4	7	NS
Retro and pelvic	8	8	
Size (cm)	9.8 ± 4.3	17.5 ± 8.3	0.008
Cell type			
Epithelioid	6	7	NS
Spindle	6	8	
Cellularity			
Low, moderate	7	8	NS
High	5	7	
Nuclear pleomorphism			
None	9	11	NS
Present	3	4	
Mitoses			
<5/50 HPF	5	7	NS
≥5/50 HPF	7	8	
MIB-1 labeling index			
<10%	10	10	NS
≥10%	2	5	
Risk grade			
Low	5	6	NS
Intermediate	5	5	
High	2	4	

NS, not significant.

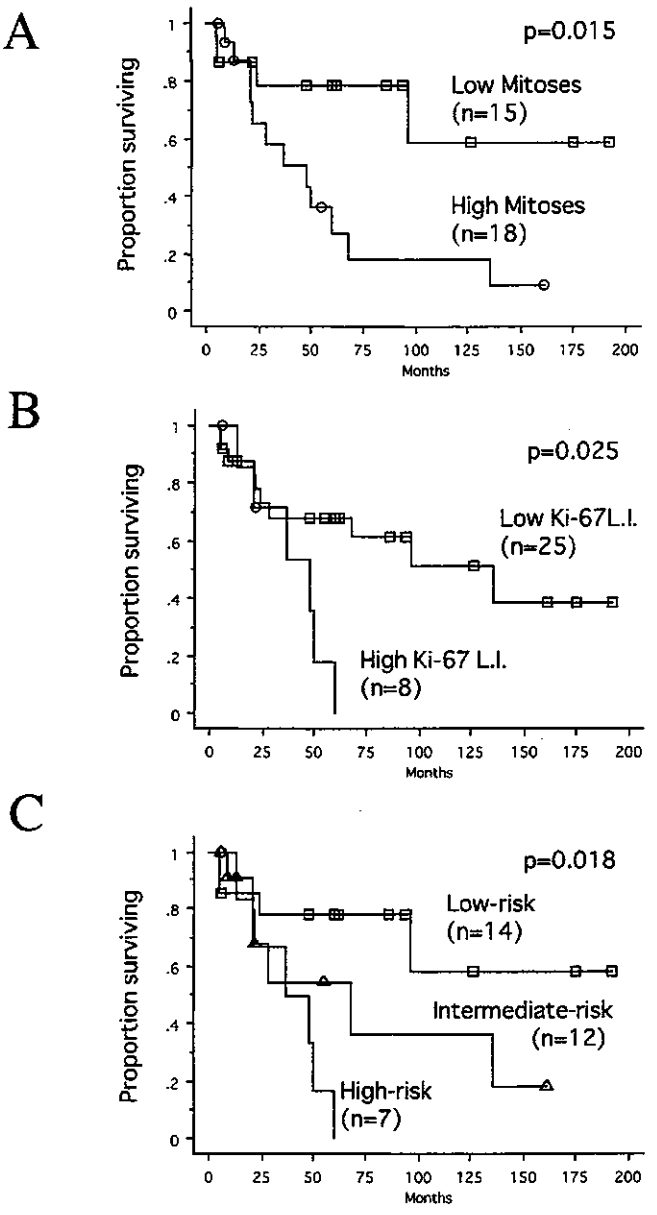

FIGURE 5. Kaplan-Meier analysis for survival. **A:** Tumors with high mitotic counts (≥5/50 HPF) have significantly shorter disease-specific survival than those with low counts (<5/50 HPF) ($P = 0.015$). **B:** Tumors with a high Ki-67 labeling index (≥10% HPF) also have a significantly shorter disease-specific survival than those with a low index (<10%) ($P = 0.025$). **C:** The high-risk group has a significantly worse prognosis ($P = 0.018$).

(31%–71%), exon 9 (3%–13%), exon 13 (0%–4%), and exon 17 (0%–4%).[1,16,26,30,34] The percentage of c-kit mutations, in particular exon 11, varies among the groups, although it is clear that the exon 11 mutation is the most frequent event in the kit gene alternations in GIST. In addition, the frequency (48%) of c-kit mutation in our EGISTs seems to be lower than that in GISTs, particularly compared with those in recent reports.[1,26] One possible explanation is the difference in the type of tissue used for DNA extraction. Two large studies using frozen specimens have shown exon 11 mutation in about 70% of GISTs[1,26]; in contrast, several studies using formalin-fixed paraffin-embedded tissue have reported it in 50% to 60%.[16,34] Another potential factor is the methodologic differences among the studies. Rubin et al[26] examined the whole sequence of c-kit cDNA by RT-PCR and the direct sequencing method, showing kit mutation in 92% of GISTs, which is the highest percentage among the large studies. Corless et al suggested the advantage of a denaturing high-pressure liquid chromatography (D-HPLC) to detect the kit mutation.[3] To prevent to miss the mutation, we performed the electrophoresis for the SSCP analysis under three different temperature conditions (data not shown). However, the anatomic site of tumors might influence